Journal of Colloid and Interface Science 563 (2020) 291–307

Contents lists available at ScienceDirect

Journal of Colloid and Interface Science

journal homepage: www.elsevier.com/locate/jcis

Novel colloidal particles and natural small molecular surfactants co-stabilized Pickering emulsions with hierarchical interfacial structure: Enhanced stability and controllable lipolysis

Yang Wei, Zhen Tong, Lei Dai, Peihua Ma, Mengfei Zhang, Jinfang Liu, Like Mao, Fang Yuan, Yanxiang Gao *

Beijing Key Laboratory of Functional Food from Plant Resources, College of Food Science & Nutritional Engineering, China Agricultural University, Beijing 100083, China

GRAPHICAL ABSTRACT

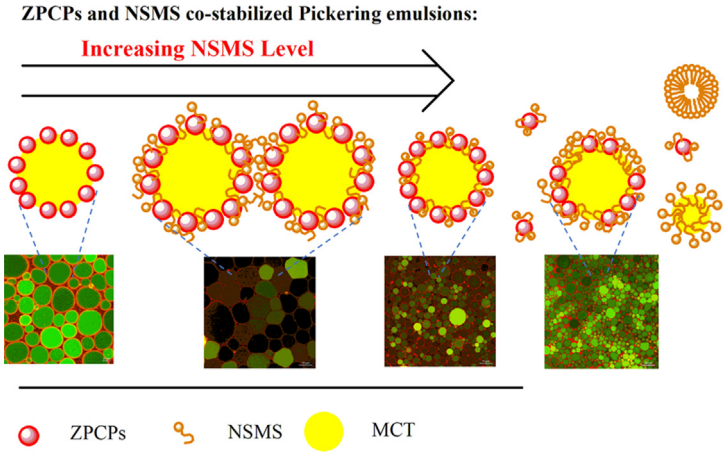

ARTICLE INFO

Article history:
Received 16 September 2019
Revised 17 December 2019
Accepted 18 December 2019
Available online 19 December 2019

Keywords:
Pickering emulsion
Small molecular surfactant
Microstructure
Stability
Rheological properties
Lipid digestion

ABSTRACT

Particle-stabilized Pickering emulsions pose several challenges to scientists researching food delivery systems. This study investigated Pickering emulsions co-stabilized by zein-propylene glycol alginate composite nanoparticles (size: 416.4 ± 8.5 nm) and rhamnolipid, quillaja saponin and tea saponin (0.01–1.00%, w/v). The results showed that different types and concentrations of natural small molecular surfactants (NSMS) had an important influence on the stability, microstructure and rheological properties of the Pickering emulsions. The surfactants were able to not only diffuse into the interfacial gaps but also adsorb onto the surface of particles to modulate the interfacial wettability, which was dependent on their types and concentrations. The negatively charged surfactants endowed the droplets with electrostatic repulsion and steric hinderance to prevent their flocculation and coalescence. In vitro digestion fate demonstrated that the presence of natural surfactants delayed the lipid digestion of the Pickering emulsions in the small intestine, particularly by decreasing the release rate of free fatty acids from 57.37% to 10.76% and 7.84% with the addition of quillaja saponin and tea saponin, respectively. The combination of

* Corresponding author at: Box 112, No.17 Qinghua East Road, Haidian District, Beijing 100083, China.
E-mail addresses: wy349@cau.edu.cn (Y. Wei), jinfang.liu@cau.edu.cn (J. Liu), likemao@cau.edu.cn (L. Mao), yuanfang0220@cau.edu.cn (F. Yuan), gyxcau@126.com (Y. Gao).

https://doi.org/10.1016/j.jcis.2019.12.085

nanoparticles and individual surfactants at the intermediate concentration (0.50%, w/v) exerted a synergistic effect on stabilizing the Pickering emulsions and inhibited lipolysis in the gastrointestinal tract, exhibiting potential applications as a fat replacer.

1. Introduction

The so-called Pickering emulsion is defined as one stabilized by solid particles at the soft interface [1–4]. An appropriate interfacial wettability of particles promotes the adsorption of particles at the interface. The ability of solid particle in adhering to the surface of droplets endows the Pickering emulsion a great resistance against coalescence or Ostwald ripening, otherwise known as the Pickering stabilizer [5]. Pickering emulsions have a wide range of applications in many areas. In terms of food product development, most of the research has focused on the synthesis of composite nanoparticles with a suitable wettability to stabilize high internal phase emulsions (HIPEs). However, it is difficult to indentify the appropriate biodegradable particles to fabricate the Pickering emulsion [6]. The complex manufacture of the stuitable particles also limits their large-scale industrial production.

Unlike particle-stabilized interfaces, surfactants are utilized to stabilize conventional emulsions by quick adsorption onto the surface of droplets and lower the interfacial tension [6]. Nonetheless, the desorption energy of low molecular weight surfactants can be less than 10 kT, which is considerably lower than that of solid particles (up to several thousand kT) [7,8]. The low interfacial adsorption energy and fragile spatial structure tend to lead the emulsion stabilized by surfactants to lose its stability during long-term storage and under different environmental stresses.

In our previous study, we investigated the effect of polymer-particle interactions on the interfacial structure and the properties of bilayer emulsions co-stabilized by zein colloidal particles and polysaccharides [9]. The synergism of polymers and particles profundly improved the physical stability of Pickering emulsions and modulated their rheology and interfacial structure. Many studies have reported on the stabilization of emulsion systems by inorganic particles (such as silica nanoparticles) and artificial surfactants [10–16]. Although these studies have revealed that the synergetic stabilizing mechanism of particles and surfactants occurs at the interface, it remains difficult to find suitable food grade surfactants to help stabilize emulsions using biocompatible colloidal particles. To the best of our knowledge, few studies have reported on edible O/W emulsions stabilized by a combination of colloidal particles and natural surfactants.

Two questions exist regarding whether the stability of Pickering emulsions co-stabilized by particles and individual surfactants can be improved and how the type and concentration of different surfactants modulates the interfacial structure of droplets, which itself influences the digestion behaviour and lipid hydrolysis of Pickering emulsions. On the one hand, ionic particles are adsorbed at the interface and provide steric hinderance and electrostatic repulsion. Natural small molecular surfactants (NSMS) are also quickly adsorbed at the interface and lower interfacial tension effectively. Therefore, the advantages of both particles and NSMS can be combined to stabilize Pickering emulsions. On the other hand, the key to lipid hydrolysis in the small intestine is the fact that bile salts are able to replace the original adsorbents through competitive adsorption, such that lipase/colipase is adsorbed onto the surface of emulsion droplets and hydrolyses lipids to form free fatty acids [17–19]. The Pickering emulsion is an excellent alternative to fat replacers since the particles on the interface are difficult to replace by bile salts [19]. However, many gaps remain between the particles at the interface, and the bile salts are still adsorbed to these binding sites. Biocompatible particles can become denatured under the gastrointestinal environment, resulting in the potential desorption of particles. The addition of NSMS could fill the interfacial gaps between the particles, thus inhibiting the adsorption of bile salts and lipid hydrolysis [20,21].

Zein, a distinct amphiphilic plant protein, can be self-assembled into colloidal particles to encapsulate nutraceuticals thanks to its intrinsic hydrophobicity, with a composition of over 50% hydrophobic amino acids [22]. Propylene glycol alginate (PGA) is generally used to fabricate protein-polysaccharide complexes with zein as a particle carrier for the delivery of nutraceuticals, otherwise known as a Pickering stabilizer [23–25]. Rhamnolipid (Rha) is a microbial surfactant, which is a typical type of glycolipid containing one or two polar rhamnose units and a non-polar fatty acid chain [26]. Rha is traditionally used for the delivery of hydrophobic molecules through a fully biodegradable transport system or the preparation of stable nanoemulsions [27]. Saponins are surface-active compounds consisting of hydrophilic sugar moieties and a hydrophobic steroid or triterpene backbone [28]. Quillaja saponin (QS) is an effective emulsifier used in the formation of nanoemulsions [29–31]. Camellia seed has been reported to be a rich source of tea saponin (TS), which can be utilized to stabilize emulsions as a natural surfactant [31]. The molecular structures of these different surfactants are illustrated in Fig. S1.

Herein, we fabricated novel Pickering emulsions co-stabilized by particles and three different types of NSMSs (Rha, QS and TS). The properties of the particles and Pickering emulsions were presented, followed by the evaluation of interfacial structure, rheological properties, stability under various environmental stresses and *in vitro* digestion of the Pickering emulsions using optical microscopy, confocal laser scanning microscopy (CLSM), cryogenic-scanning electric microscopy (cryo-SEM) and other analytical methods. The impact of the different combinations of composite nanoparticles and NSMSs at the interface on the stability, microstructure and lipid hydrolysis was investigated. Our results provide a theoretical basis for the design of nutraceutical Pickering emulsions in the future.

2. Materials and methods

2.1. Materials

Zein (protein content: 91.3%) was obtained from Sigma-Aldrich. Propylene glycol alginate (PGA) was generously provided by Hanjun Sugar Industry Co. Ltd. (Shanghai, China). Medium-chain triglycerides (MCT, Miglyol 812 N) were from Musim Mas (Medan, Indonesia). Rhamnolipid (≥90%) was obtained from Parnell Biological Technology Co. Ltd (Shaanxi, China). Tea saponin (TS) was donated by Han Qing Biological Technology Co. Ltd. (Hunan, China), which was supplied as a yellowish powder that contains around 51.8% saponin, 36.1% total carbohydrate, 5.6% crude protein, 2.7% ash, and 3.7% water. Quillaja saponin (QS) is a heterogenous mixture of molecules varying both in their aglycone and sugar moieties, which was reported to have about 35% sapogenin content from Sigma-Aldrich. Absolute ethanol (99.99%), solid

sodium hydroxide and liquid hydrochloric acid (36%, w/w) were acquired from Eshowbokoo Biological Technology Co.,Ltd. (Beijing, China).

2.2. Sample preparation

2.2.1. Preparation of ZPCPs and different NSMS solutions

Zein-PGA composite particles (ZPCPs) were prepared by the solvent-evaporation co-precipitation method according to our previous study with some modifications.[24] Briefly, 2.7 g zein and 0.3 g PGA were co-dissolved in 1000 mL 70% (v/v) aqueous ethanol solution and stirred at 600 rpm overnight at 25 °C to make sure that they were completely dissolved. Thereafter, the ethanol was removed using a rotary evaporator at 45 °C for 60 min and the remaining volume was set to around 250 mL. The colloidal dispersion was diluted with pH-adjusted water (pH 4.0) to 300 mL. The ZPCPs were centrifuged (Sigma 3 k15, Germany) at 3000 rpm for 10 min to separate any large particles and aggregates. Finally, the supernatant was adjusted to pH 4.0 using 0.1 M HCl solution. Part of ZPCPs was placed at 5 °C for further analysis, while the other part was freeze-dried for 72 h to obtain powder samples. Different NSMS solutions at various concentrations (0.01%, 0.05%, 0.10%, 0.25%, 0.50%, 0.75% and 1.00%, w/v) were prepared by dissolving NSMSs in deionized water and stirring at 600 rpm overnight to warrant complete hydration. Then pH was adjusted to 4.0 with 1 M NaOH.

2.2.2. Preparation of Pickering emulsions co-stabilized by ZPCPs and NSMSs

Briefly, the primary emulsion (the ZPCPs stabilized Pickering emulsion) was prepared by mixing 7.5 mL of the ZPCPs (2.0%, w/v) dispersion with 15 mL of oil phase (MCT) at 15000 rpm using a blender (Ultra Turrax, model T25, IKA Labortechnic, Staufen, Germany). After the complete addition of MCT, the mixture was further homogenized for another 5 min to obtain the primary emulsion. Secondary emulsions (the ZPCPs/NSMS co-stabilized Pickering emulsions) were obtained by mixing the primary emulsion with 7.5 mL of individual NSMS solutions (0.01–1.00%, w/v). The different ZPCPs and Rha co-stabilized Pickering emulsions were termed as Z-P/0.01rha, Z-P/0.05rha, Z-P/0.10rha, Z-P/0.25rha, Z-P/0.50rha, Z-P/0.75rha and Z-P/1.00rha, respectively. The different ZPCPs and TS co-stabilized Pickering emulsions were termed as Z-P/0.01ts, Z-P/0.05ts, Z-P/0.10ts, Z-P/0.25ts, Z-P/0.50ts, Z-P/0.75ts and Z-P/1.00ts, respectively. The different ZPCPs and QS co-stabilized Pickering emulsions were termed as Z-P/0.01qs, Z-P/0.05qs, Z-P/0.10qs, Z-P/0.25qs, Z-P/0.50qs, Z-P/0.75qs and Z-P/1.00qs, respectively. The Pickering emulsion stabilized by ZPCPs solely was termed as Z-P. Besides, 0.10%, 0.50% and 1.00% (w/v) of NSMS solutions (Rha, TS and QS) were selected to prepare traditional emulsions solely as control groups, which were termed as 0.10rha, 0.50rha, 1.00rha, 0.10ts, 0.50ts, 1.00ts, 0.10qs, 0.50qs and 1.00qs, respectively.

2.3. Particle properties

2.3.1. Particle size, zeta (ζ)-potential, and polydispersity index (PDI) of ZPCPs

The particle size (Z-average size), zeta-potential, and PDI of the composite particles were analysed using a Zetasizer (Nano-ZS90, Malvern Instruments Ltd., Worcestershire, UK) with a DTS1060 cuvette at a scattering angle of 90°. Samples were diluted tenfold in distilled water (pH 4.0) to prevent multiple light scattering effects. Thereafter, the samples were adjusted to pH 4.0 to determine the particle size and zeta-potential. All measurements were conducted in triplicate.

2.3.2. Wettability measurement of ZPCPs

The contact angle (θo/w) of the ZPCPs was determined using an OCA 20 AMP (Dataphysics Instruments GmbH, Germany) according to the method described in our previous study.[32] All the measurements were conducted in triplicate and averaged.

2.3.3. Field emission scanning electron microscopy (FE-SEM)

The morphology of composite nanoparticles was observed using a field emission scanning electron microscopy (FE-SEM, SU8010, Hitachi). The samples were placed on a double-sided coat with a thin layer of gold and measured under an acceleration voltage of 20.0 kV [33].

2.4. Size and surface charge of oil droplets

Twelve hours after the preparation of the Pickering emulsions, the droplet size was measured using a laser scattering size analyser (LS230®, Beckman Coulter, USA). Under continuous stirring at 3000 rpm, the emulsions were diluted until an obscuration rate between 8% and 12% was obtained. The parameters were applied as followed: a refractive index of 1.52 for MCT and an absorption of 0.001, and a refractive index of 1.33 for the dispersant (deionized water) [6]. The volume-area ($D_{4,3}$) average diameters were calculated using the following equation:

$$D4,3 = \frac{\sum nidi^4}{\sum nidi^3}$$

where n_i is the number of particles with a diameter of d_i.

The electrical properties of the droplets were determined using a Zeta sizer NanoZS90 (Malvern Instruments, Worcestershire, UK). The Pickering emulsions were diluted to 0.005 wt% with pH-adjusted water (pH 4.0) to minimize multiple scattering effects. Data were collected from at least 10 sequential readings per sample after 120 s of equilibration and calculated using the Smoluchowski model [32]. All measurements were performed in triplicate.

2.5. Interfacial tension measurement

The interfacial tension between the aqueous phase (NSMS solutions, Z-P dispersion and Z-P/NSMS mixed dispersions) and oil phase (MCT) was measured using a Tensiometer K100 (Kruss, Germany) according to the method reported by O'Sullivan et al. (2014) [34]. The Wilhelmy plate was made of platinum, with a length, width and thickness of 19.9 mm, 10 mm and 0.2 mm, respectively. The Wilhelmy plate was immersed in 20 g of aqueous phase to a depth of 3 mm with a surface detection speed of 15 mm/min and maintained at 20 °C. The interfacial tension values and error bars were reported as the average and the standard deviation of three replicates, respectively.

2.6. Observation of interfacial structure

2.6.1. Optical microscopy

The microstructure of the Pickering emulsions was observed at 25 °C with an optical microscope (Leica DMD 108, Leica Microsystems Inc., Heidelberg, Germany) equipped with a camera. An aliquot of the emulsion was placed at the centre of a slide glass and covered with a cover glass [35].

2.6.2. Confocal laser scanning microscope (CLSM)

Confocal laser scanning microscopy (CLSM) (Zeiss780, Germany) was used to visualize the interfacial structure of the oil droplets. Nile blue (0.1%, w/v) was used to stain the ZPCPs, while Nile red (0.1%, w/v) was used to dye the oil phase (MCT).

The dyed emulsions were then deposited on concave confocal microscope slides and gently covered with a cover slip. The CLSM was operated using two laser excitation sources: an argon/krypton laser at 488 nm (Nile red) and a Helium Neon laser (He-Ne) at 633 nm (Nile blue).

2.6.3. Cryo-SEM

In the Cryo-SEM technique, the sample was vitrified with liquid nitrogen and maintained at a very low temperature. The structure of the Pickering emulsions was thereby preserved in a frozen state, allowing them to remain stable during the observation of their microstructure [36]. The microstructure of the Pickering emulsions co-stabilized by ZPCPs and different NSMSs was observed using Cryo-SEM. The samples were placed on an aluminum plate, and transferred to a cryo-preparation system (PP3010T, Quorum Inc., UK) to flash-freeze the samples in liquid nitrogen slush followed by high vacuum sublimation of unbound water. The samples were freeze-fractured in the cryo-preparation chamber and coated with platinum. Images were captured using SEM (Helios NanoLab G3 UC, FEI, USA). The analysis was performed at a working distance between 3 and 5 mm with TLD detection at 2 kV.

2.7. Physical stability

The physical stability of the emulsions was measured by a LUMiSizer (L.U.M. 290 GmbH, Germany), using centrifugal sedimentation to accelerate the occurrence of instability phenomena such as sedimentation, flocculation, and creaming [35]. The samples were subjected to centrifugal force, and then illuminated with near-infrared light to assess the intensity of the transmitted light as a function of time and position over the entire sample length, simultaneously. The parameters used for the measurement were set as follows: 1.2 mL of the emulsion; rotational speed, 3000 rpm; performed time, 3600 s; time interval, 20 s; temperature, 25 °C.

2.8. Storage stability

After the preparation of the emulsions, the droplet size and zeta-potential were measured and recorded at regular storage intervals (1, 7, 14, 21 and 28 days). The visual characteristics of the emulsions during different storage periods were also observed.

2.9. Rheological properties

The rheological properties of the emulsions were determined at 25 °C using an AR-1500 rheometer (TA Instruments, West Sussex, UK) with a steel parallel plate (40 mm diameter, gap 0.100 mm). The samples were deposited onto the plate and allowed to reach temperature equilibrium for 5 min. For the steady-state flow measurement, the shear rate ranged from 0.1 to 100 s^{-1}, with the apparent viscosity (η) obtained from TA data analysis software. All the dynamic tests were performed within the linear viscoelastic region, and a stress value of 1 Pa was chosen for the frequency test. Frequency was oscillated between 0.1 and 100 rad/s and strain was performed at 1% [37]. Both elastic modulus (G′) and loss modulus (G″) were recorded versus frequency to determine whether the emulsion was strongly or weakly flocculated. All measurements were performed in triplicate.

2.10. Environmental stability

2.10.1. Effect of pH

The effect of pH on the emulsion stability was evaluated according to the method of Wei et al. [37]. The experimental emulsions after 12 h of storage at ambient temperature (25 °C) were adjusted to pH 2.5, 6.0 and 8.5 using either 0.1 M NaOH or 0.1 M HCl.

2.10.2. Effect of ionic strength

The emulsions after 12 h of storage at ambient temperature (25 °C) were mixed with different quantities of NaCl powder for 2 h to ensure uniform dispersion and complete dissolution. The NaCl concentrations in the different emulsion samples were adjusted to then 10, 50 and 100 mM [27].

2.10.3. Effect of thermal treatment

The emulsions after 12 h storage at ambient temperature (25 °C) were incubated in water bath (85 °C) for 60 min and then cooled down to 25 °C [37].

After each treatment, the average droplet size, size distribution and zeta-potential of the emulsions were evaluated after 12 h storage (25 °C).

2.11. In vitro digestion analysis and free fatty acid release

An *in vitro* gastrointestinal model was applied according to a modified procedure described in our previous study: [33].

Stomach phase: Briefly, 20 mL of the emulsion was mixed with 20 mL of simulated gastric fluid (SGF) containing 0.0032 g/mL pepsin to mimic gastric digestion. The pH was adjusted to 2.0 and the sample was then swirled at 150 rpm for 1 h at 37 °C.

Small intestine phase: Briefly, 20 mL of gastric digesta was transferred into a 100 mL glass beaker and then adjusted to pH 7.0. Thereafter, 20 mL of simulated intestinal fluid (SIF) containing 5 mg/mL bile salt, 0.4 mg/mL pancreatin and 3.2 mg/mL lipase was mixed with digesta. The pH was adjusted to 7.0 and the samples were held under continuous vibration at 150 rpm for 2 h at 37 °C to mimic small intestine digestion.

The degree of lipolysis was measured according to the amount of free fatty acids (FFAs) released. The quantity of 0.25 M NaOH required to neutralize the released FFAs through lipid digestion was determined on a pH-stat automatic titration unit (Metrohm, Switzerland, 916 Ti-Touch) [21]. The digestion of ZPCPs-stabilized Pickering emulsions and individual NSMS-stabilized conventional emulsions was also carried out as control groups. The quantity of FFAs released was determined as the percentage of FFA (%) released during the digestion period as described by Li and McClements:[38]

$$\%FFA = 100 \times \frac{V_{NaOH} m_{NaOH} M_{lipid}}{2W_{lipid}}$$

where V_{NaOH} and m_{NaOH} represent the volume (L) and concentration (M) of NaOH solution needed to neutralize the FFAs, and W_{lipid} and M_{lipid} represent the initial mass (g) and molecular mass ($g{\cdot}mol^{-1}$) of the triacylglycerol.

2.12. Statistical analysis

All the data obtained were average values of triplicate determinations and subjected to statistical analysis of variance using SPSS 18.0 for Windows (SPSS Inc., Chicago, USA). Statistical differences were determined by one-way analysis of variance (ANOVA) with Duncan's post hoc test and least significant differences ($p < 0.05$) were accepted among the treatments.

3. Results and discussion

3.1. Characteristics of ZPCPs

ZPCPs were prepared using the solvent-evaporation co-precipitation according to our previous study with some modifications [24,33]. The mean hydrodynamic size and polydispersity index (PdI) of ZPCPs were 416.4 ± 8.5 nm and 0.222 ± 0.029, respectively (Fig. 1A). This result showed that ZPCPs were markedly big-

ger than the inorganic nanoparticles used in the stabilization of Pickering emulsions [12,13,25]. The large size of the particles could provide sufficient energy for attachment at the oil–water interface [2,7,8]. The isoelectric point (pI) of zein is around pH 6.2 and PGA has a dissociation constant (pKa) around pH 3.5 [23]. Therefore, zein can successfully integrate with PGA at pH 4.0 via electrostatic attraction to form ZPCPs. ZPCPs had a negative charge (−13.97 ± 0.05 mV). Although the particles could hardly provide sufficient electrostatic repulsion among the droplets, they showed a long-term stability against coalescence and Ostwald ripening due to the steric hinderance [25].

The interfacial wettability of the particles plays a crucial role in Pickering stabilization [35]. Adequate wettability is an important prerequisite for the adsorption of particles at the oil-in-water interface, which is determined by the contact angle ($\theta_{o/w}$). The $\theta_{o/w}$ of ZPCPs was around 73.0 ± 0.4° (Fig. 1B), which may be attributed to more hydrophilic residues exposed to the surface of particles during the process of solvent-evaporation co-precipitation.

The morphology of ZPCPs was observed by FE-SEM (Fig. 1C). ZPCPs exhibited a spherical shape with a diameter of around 400 nm, which was consistent with the result of DLS. Although the suitable wettability and regular sphericity could promote the particles to be adsorbed on the surface of droplets, the large size

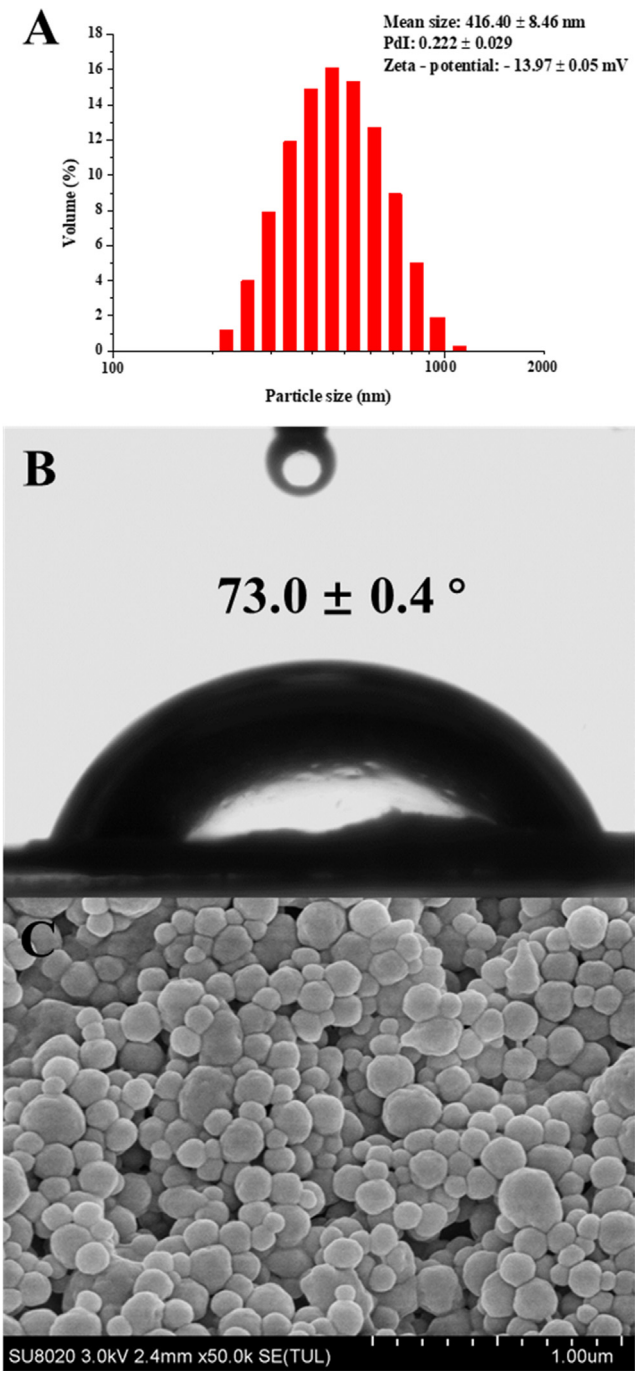

Fig. 1. Particle size distribution (A), interfacial wettability (B) and morphology (C) of zein-PGA composite nanoparticles.

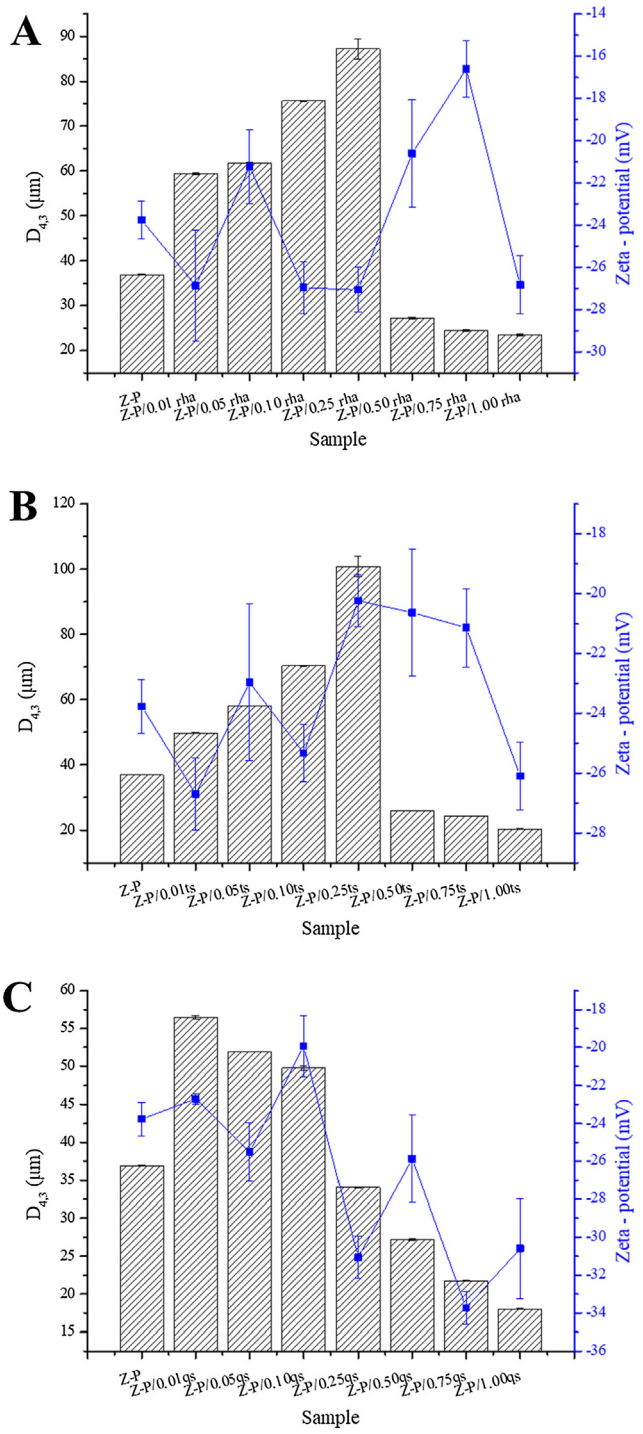

Fig. 2. Droplet size and zeta-potential of Pickering emulsions co-stabilized by zein-PGA composite nanoparticles and individual Rha (A), TS (B) or QS (C).

would reduce the adsorption rate of the particles onto the interface and leave large interfacial gaps between the particles [7,39].

3.2. Size distribution and zeta-potential of oil droplets

As shown in Fig. 2A, the droplet size of the Pickering emulsion stabilized by the particles solely was 36.92 ± 0.04 μm. However, it was continuously increased when a low quantity of Rha was added to the Pickering emulsion. The droplet size of the Pickering emulsion co-stabilized by ZPCPs and Rha reached its maximum (87.19 ± 2.26 μm) at Z-P/0.25rha, which indicated that the addition of Rha promoted the aggregation of droplets and reduced the stability of the Pickering emulsion.

When the concentration of Rha reached 0.50% (w/v), there was a marked reduction in the droplet size of the Pickering emulsion co-stabilized by ZPCPs and Rha. Solid particles and surfactants have two distinct mechanisms to stabilize the emulsion: the particles can either be adsorbed at the interface due to their suitable wettability and stabilize the droplets by steric hindrance and electrostatic repulsion, surfactants can be quickly adsorbed at the droplet surface, effectively reducing the interfacial tension due to their amphiphilic structure and low molecular weight [31]. According to the measured interfacial tension in Fig. S3, Rha would be adsorbed at the gaps among the particles on the surface of oil droplets, significantly reducing the interfacial tension between the oil and water, allowing large droplets to further break down during emulsification to form smaller droplets. Rha has a carboxylic acid group as part of the hydrophilic head group and a hydrocarbon chain as a non-polar tail (Fig. S1A) with the excellent surface-activity [40]. The addition of Rha altered the interfacial composition of the droplets and formed a more compact adsorbed layer [41]. Similarly, Binks and Rodrigues found a synergistic behaviour between particles and surfactants when stabilizing the emulsion [39]. The minimum size of the Pickering emulsion obtained at Z-P/1.00rha was 23.46 ± 0.20 μm, which was markedly smaller than that of Z-P. Meanwhile, the zeta-potential was reversely decreased from −16.60 ± 1.35 to −26.83 ± 1.38 mV. In spite of the high desorption energy of the particles on the droplet surface, nanoparticles and surfactants were still able to undergo competitive adsorption at the mixed interface, which exhibited a profound influence on the interfacial structure [42]. An apparent reduction in the zeta-potential of droplets indicated that a part of nanoparticles at the interface was replaced by Rha molecules.

Fig. 2B demonstrated the influence of TS on the droplet size and the zeta-potential of the Pickering emulsion. The addition of TS into the particle-stabilized emulsion resulted in the occurrence of larger droplets initially possibly due to the bridging of the particles adsorbed at the interface, which was also similar to the effect of Rha [39]. A similar phenomenon was observed in the droplet size of the Pickering emulsion. When the concentration of TS was above 0.25% (w/v), the droplet size of the emulsion was continuously decreased with the rise of TS level. Nevertheless, the droplet size of the Pickering emulsion co-stabilized by ZPCPs and TS was notably larger than that co-stabilized by ZPCPs and Rha. As shown in Figs. S3 and S4, Rha had a higher efficiency in lowering the interfacial tension than TS, whether at a single surfactant interface or a mixed particle-surfactant interface. This could be ascribed to the fact that Rha has a lower molecular weight than TS, and is therefore more easily adsorbed to the interfacial gaps between the particles (Fig. S1). Saponin is a structurally diverse class of amphiphilic glycosides and occurs in various plants. Based on its molecular structure, TS is a highly surface-active surfactant consisting of a hydrophobic aglycone part and a hydrophilic carbohydrate part [31].

With the addition of QS, the droplet size of the Pickering emulsion co-stabilized by ZPCPs and QS was markedly increased initially, which was similar to Rha and TS. However, there was a continuous reduction in the droplet size of the emulsion with a rise in the QS levels. The majority of Quillaja saponins contain quillaic

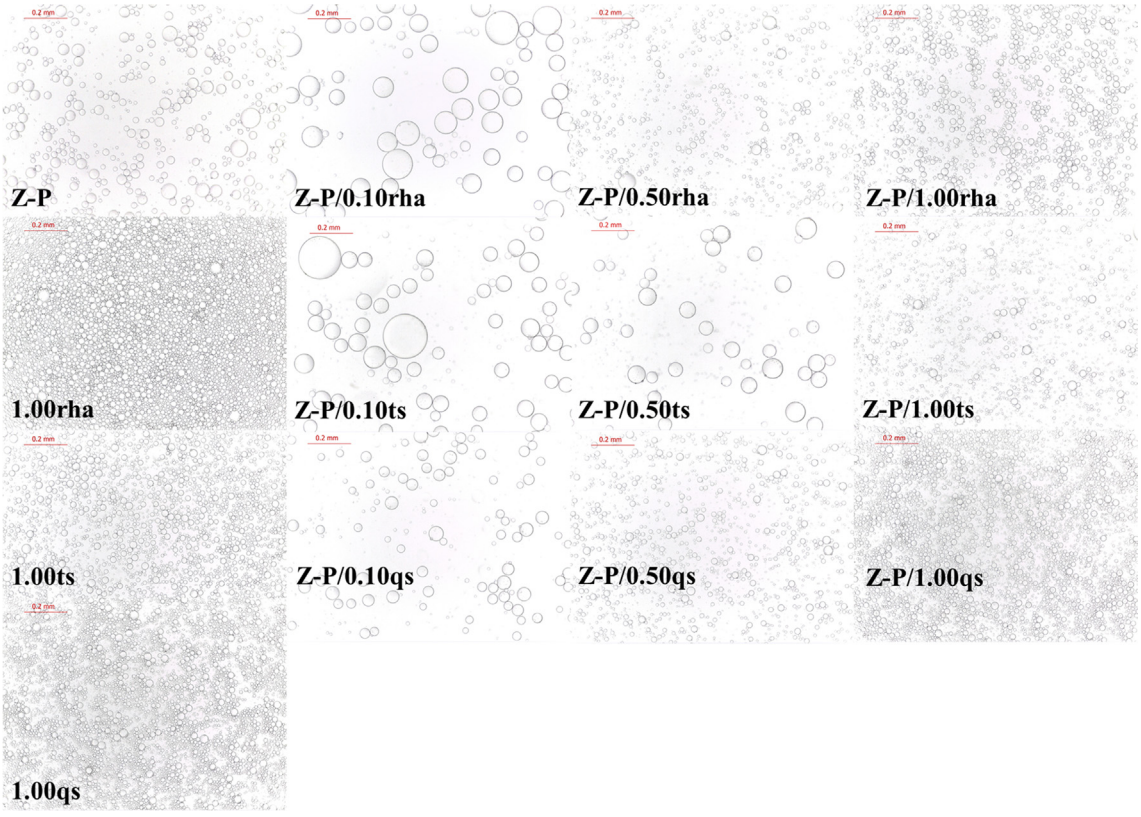

Fig. 3. Optical microscope images of Pickering emulsions co-stabilized by ZPCPs and individual Rha, TS and QS.

acid as the triterpene backbone, which is linked to a di- or trisaccharide at the C3-positionand esterified with a complex oligosaccharide (which may be acetylated) at position C28 [29]. Overall, the droplet size of the Pickering emulsion co-stabilized by ZPCPs and QS was significantly ($p < 0.05$) smaller than that of the ZPCPs and Rha or TS co-stabilized Pickering emulsion. As shown in Figs. S3 and S4, QS reduced the interfacial tension more effectively than Rha and TS. Based on its large molecular weight (Mw: 1650) and strong interfacial adsorption capacity, QS could considerably enhance the stability of the Pickering emulsion by elevating the adsorption rate and providing steric hindrance. When a low level of surfactants was added to the particle-stabilized interface, they could interact with the nanoparticles and be adsorbed onto the surface of the nanoparticles. Meanwhile, the NSMS adsorbed on the surface of the nanoparticles also acted as a bridge between the nanoparticles, strengthening the attraction between them, resulting in the aggregation of the droplets [43].

3.3. Optical microscopy

Optical microscopy was used to observe the morphology of the droplets in the Pickering emulsions. The droplets in all the samples showed a regular spherical shape with different dimensions (Fig. 3). The presence of surfactants caused different magnitudes of aggregation of the particle-stabilized droplets and an increase in the droplet size. With the addition of NSMS at a low concentration, several larger droplets were observed at Z-P/0.10rha and Z-P/0.10ts. Comparably, the droplet size of Z-P/0.10qs was more uniform and smaller. The optical observation of the emulsion was consistent with its droplet size distribution. When the concentration of surfactants was increased, the emulsion gradually exhibited a more uniform and smaller droplet size. As the concentration of NSMS reached 1.00% (w/v), the morphology of the Pickering emulsion co-stabilized by ZPCPs and NSMS was similar to the traditional emulsions solely stabilized by individual surfactants.

3.4. CLSm

CLSM was used to observe the interfacial structure of the Pickering emulsions by marking the composite particles and oil phase. Z-P showed the typical spherical droplets with a shell of particle phase, and the dense nanoparticles were adsorbed at the surface of the droplets with the steric hinderance and electrostatic repulsion to stabilize the Pickering emulsion (Fig. 4). The low levels of

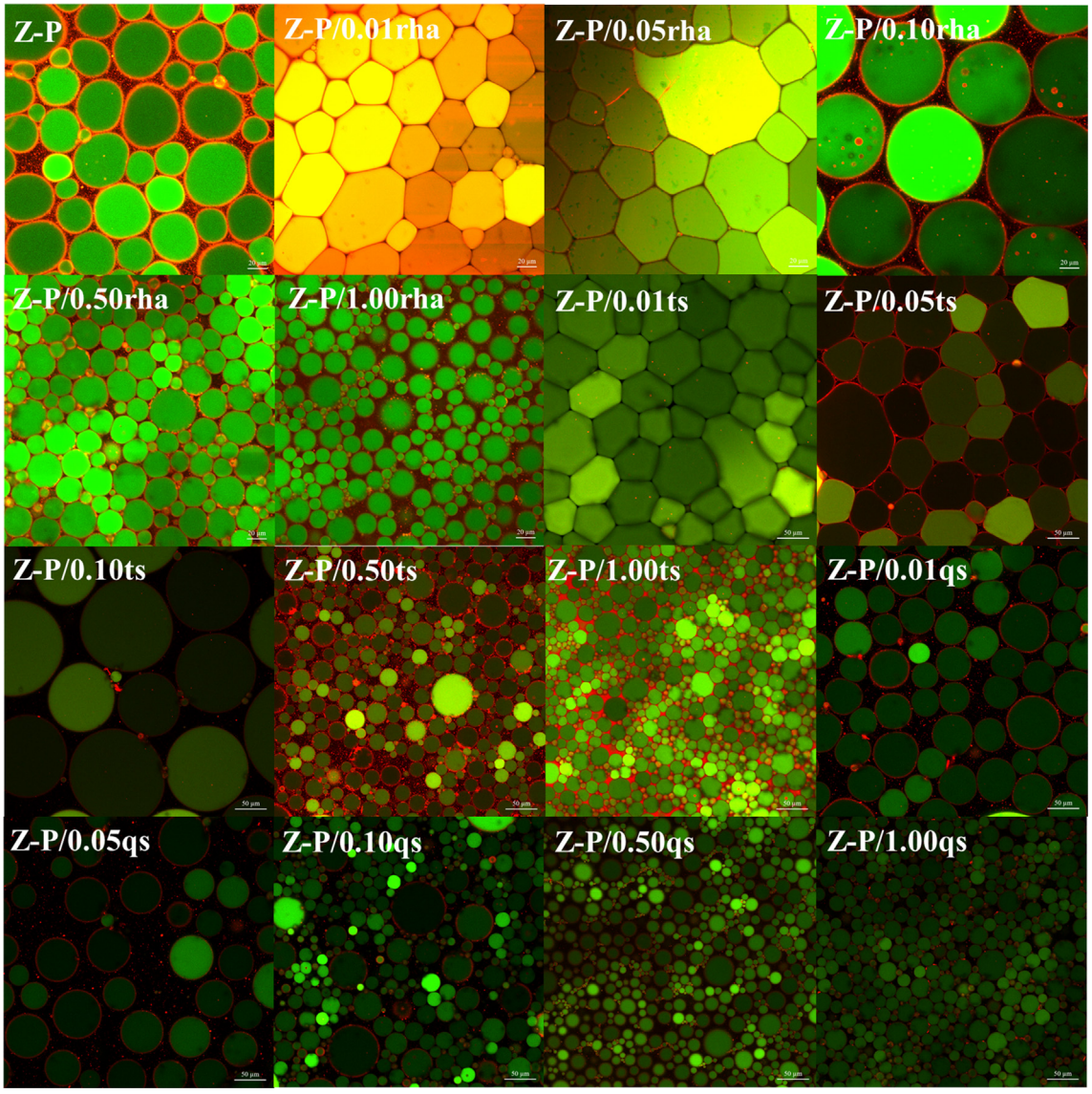

Fig. 4. CLSM images of Pickering emulsions co-stabilized by zein-PGA composite nanoparticles and individual Rha, TS and QS.

Rha (0.01% and 0.05%, w/v) resulted in a severe deformation and aggregation of the droplets. The morphology of the droplets was changed from a spherical shape to closely packed cell wall. A low level of Rha resulted in a bridging between the droplets or the adsorption onto the surface of particles to further increase the hydrophilicity, which would also produce the bridging effect [10,27,42]. With the rise of Rha concentration, the droplet size of the Pickering emulsion decreased continuously and the droplets were separated. Moreover, it was observed that the part of particles was desorbed from the interface of droplets at Z-P/1.00rha, which was attributed to the competitive adsorption and displacement between ZPCPs and Rha at the interface [12,39]. A similar phenomenon was found in the ZPCPs and TS co-stabilized Pickering emulsion. The addition of TS led to a severe aggregation of droplets, however, the droplet size was progressively reduced with an increase in the TS levels. Comparably, the ZPCPs and QS co-stabilized Pickering emulsion exhibited a better physical stability. At a low concentration of QS, the particle layer was adsorbed around the droplets to provide effective steric hindrance. At a high concentration of QS, surfactant domains formed on the surface of the droplets, squeezed the areas of nanoparticles, and elevated the surface pressure, leading to the aggregation of nanoparticles at the interface [42].

3.5. Cryo-SEM

Cryo-SEM was used to analyze the original structure of the Pickering emulsions and their interfacial properties. The spherical

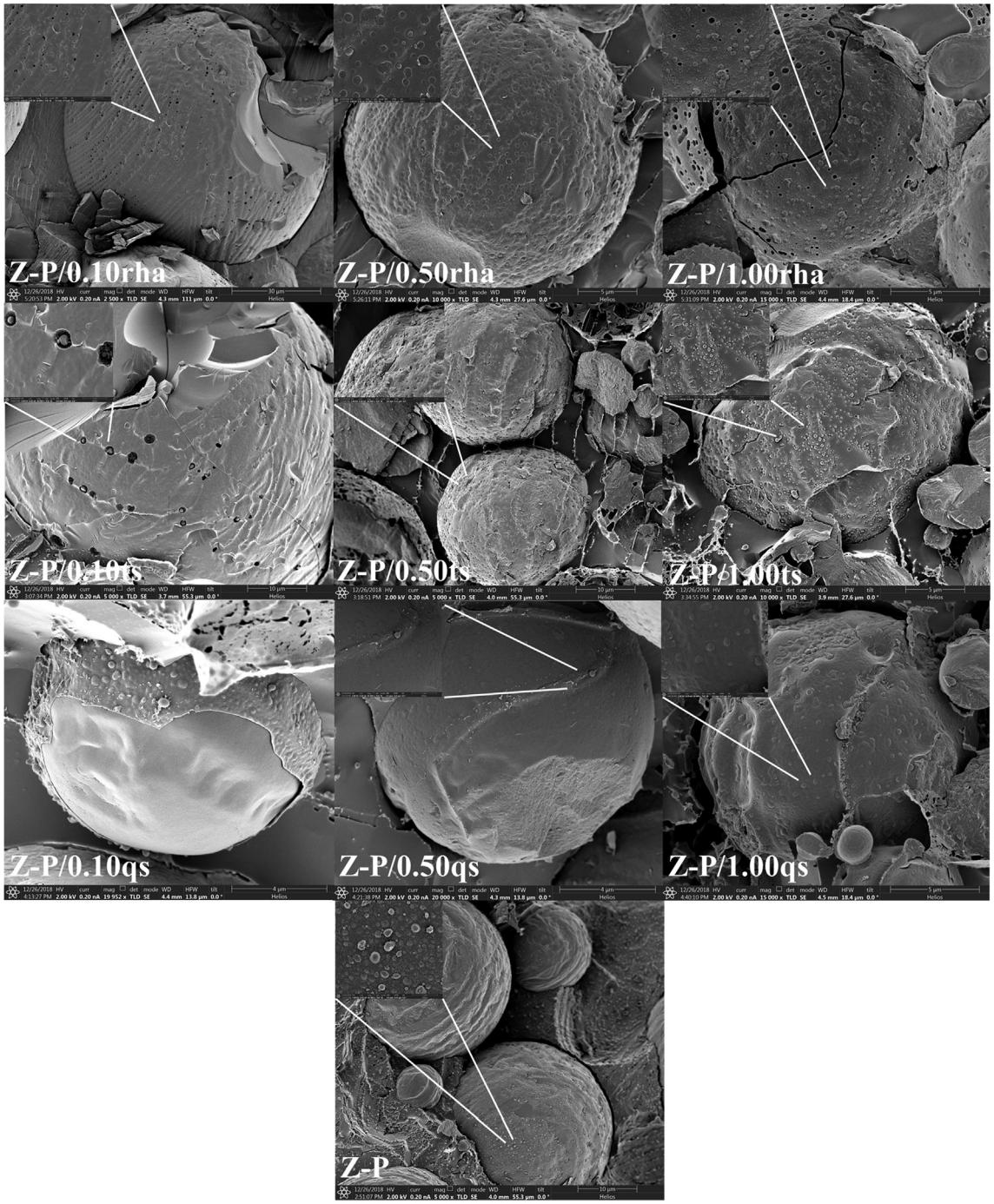

Fig. 5. Cryo-SEM microstructure of Pickering emulsions co-stabilized by ZPCPs and individual Rha, TS or QS.

droplets were observed in the frozen emulsions (Fig. 5). Different quantities of nanoparticles were adsorbed and distributed on the surface of the droplets. Due to strong hydrophilicity, only a small part of the ZPCPs were able to enter into the oil phase, and most were wetted by the aqueous phase, which is presented in the insert image of Z-P. On the one hand, with the addition of different NSMSs, they adsorbed onto the surface of nanoparticles and altered the interfacial wettability of particles [44]. According to the images of Z-P/1.00rha, Z-P/1.00ts, and Z-P/1.00qs, when the surfactant concentration was higher, the particles adsorbed onto the surface of the droplets were embedded deeper into the oil phase, indicating that the hydrophobicity of the particles was enhanced. On the other hand, according to observations using cryo-SEM, a high level of NSMS significantly increased the density of the particles adsorbed at the interface, and a number of interfacial pores appeared on the droplet surface. The size of these pores was consistent with that of particles previously adsorbed on the droplet surface, which confirmed that the addition of surfactants indeed caused the aggregation of particles and a competitive displacement between particles and NSMS on the mixed particle/NSMS interface [14,39]. This phenomenon was pronounced in the ZPCPs and Rha co-stabilized Pickering emulsion, especially at a low concentration (0.10%, w/v) and more markedly high concentration (1.00%, w/v) of Rha. As previously mentioned, Rha has a smaller molecular structure and therefore more easily adsorbs onto the interfacial gaps. Interestingly, no more pores were observed in the droplet surface of Z-P/0.50rha, which indicated that the intermediate concentration of Rha (0.50%, w/v) had a synergistic effect on composite particles, with the resultant Pickering emulsion becoming more stable.

3.6. Physical stability

Compared to the physical stability of Z-P, the stability of the Pickering emulsion co-stabilized by ZPCPs and Rha was continuously reduced when the concentration of Rha was elevated from 0.01% to 0.25% (w/v) (Fig. 6A). However, the stability of the Pickering emulsion was improved when the level of Rha was above 0.50% (w/v). Among all of the Pickering emulsions co-stabilized by ZPCPs and Rha, Z-P/0.50rha exhibited the best stability. This finding was consistent with the observations by CLSM and cryo-SEM, since Rha and particles were co-adsorbed onto the interface and had a synergistic effect, improving the stability of the Pickering emulsions at the intermediate concentration of Rha, where neither bridging nor competitive replacement occurred. As shown in Fig. 6B, Z-P/0.01ts exhibited the worst stability among all the samples. With the rise of TS, the stability of the Pickering emulsion co-stabilized by ZPCPs and TS was enhanced. Besides, the stability of the ZPCPs and QS co-stabilized Pickering emulsion was similar to that of the ZPCPs and Rha co-stabilized Pickering emulsion. With the addition of QS at lower levels (<0.10%, w/v), the physical stability of the Pickering emulsion co-stabilized by particles and QS became worse than that of Z-P (Fig. 6C). Nevertheless, the stability of the emulsion was improved as the concentration of QS increased further and the best stability was found at 0.50% (w/v) of QS. When the level of QS continued to increase, the emulsion stability was decreased slightly. As a supplement, Fig. 6D, E and F showed the physical stability of the conventional emulsions solely stabilized by Rha, TS and QS, respectively. In summary, Z-P/0.50rha and Z-P/0.50ts showed a better physical stability than the other emulsions.

3.7. Storage stability

Among all the Pickering emulsions co-stabilized by ZPCPs and Rha, Z-P/0.25rha was the most unstable during storage period, followed by Z-P/0.10rha, Z-P/0.05rha and Z-P/0.01rha (Fig. 7A). Compared to Z-P, the storage stability of the Pickering emulsion was improved when the concentration of Rha was above 0.50% (w/v). A similar phenomenon was observed in the ZPCPs and TS co-stabilized Pickering emulsion. Z-P/0.25ts showed the worst stability among all the samples, followed by Z-P/0.10ts, Z-P/0.05ts and Z-P/0.01ts (Fig. 7B). At a higher concentration of TS, the storage stability of the Pickering emulsion was visibly enhanced. Fig. 7C showed the influence of QS level on the storage stability of the Pickering emulsion. A greater increase was observed in the droplet size of Z-P/0.01qs and Z-P/0.10qs, followed by Z-P/0.05qs and Z-P/0.25qs. However, the storage stability of the Pickering emulsion was found to be greater at a higher QS level. The zeta-potential of the majority of the emulsions exhibited irregular fluctuations, indicating that surfactants were primarily involved in the interconversion of dynamic adsorption and desorption [41–43]. Moreover, an

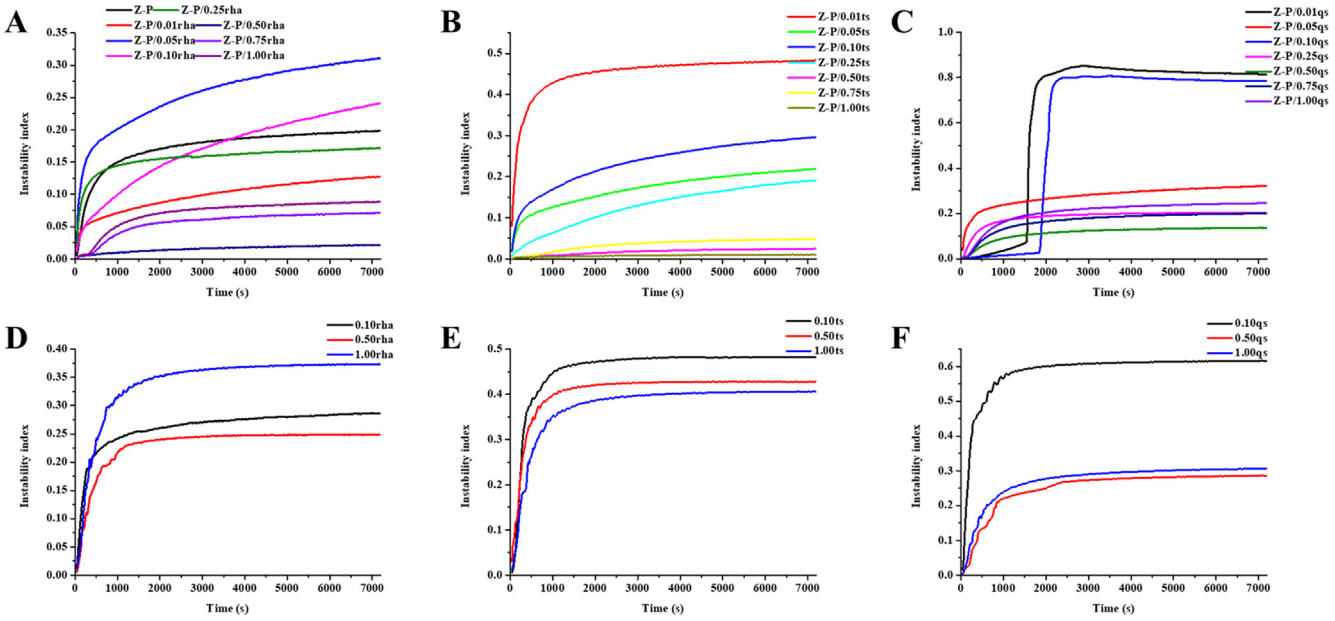

Fig. 6. Physical stability of Pickering emulsions co-stabilized by zein-PGA composite nanoparticles and Rha (A), TS (B) or QS (C), physical stability of nanoemulsions stabilized by individual Rha (D), TS (E) or QS (F).

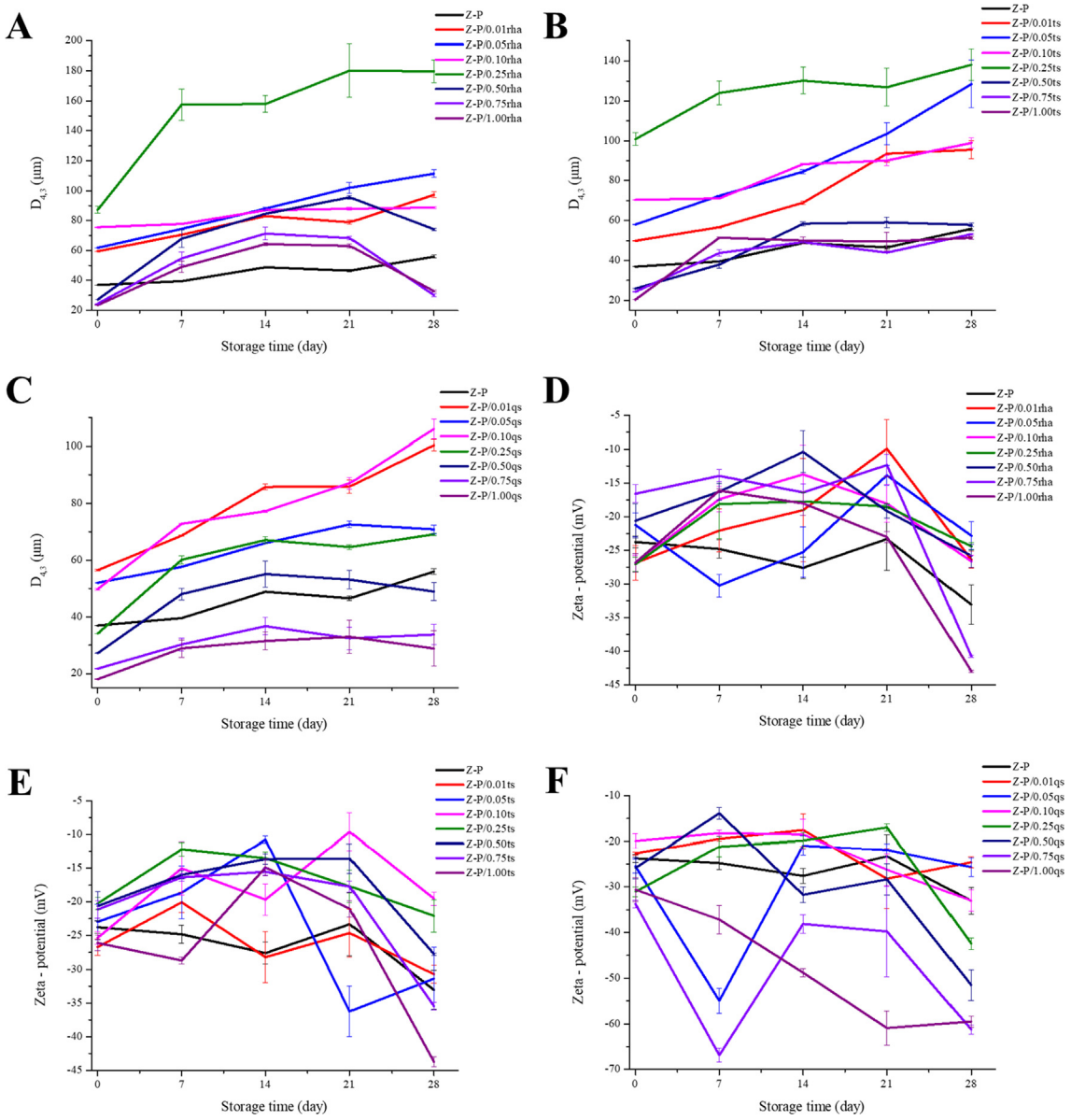

Fig. 7. Effect of storage period on the droplet size of Pickering emulsions co-stabilized by ZPCPs and Rha (A), TS (B) or QS (C), effect of storage period on zeta-potential of Pickering emulsions co-stabilized by ZPCPs and individual Rha (D), TS (E) or QS (F).

interesting phenomenon was observed in the final week of the storage period: the droplet size of part of the Pickering emulsions co-stabilized by particles and Rha or QS decreased slightly, particularly in the higher levels of NSMS (0.75% and 1.00%, w/v). Presumably, the excessive Rha or QS molecules diffused into the interfacial pores between the particles and induced competitive displacement between the particles and surfactants [12,39,42]. On the one hand, the desorption of the particles from the interface broke the bridging flocculation between the droplets, which separated the droplets from each other [39,41,43]. On the other hand, after a long period of storage, the NSMS originally adsorbed onto the surface of particles could be desorbed, thereby altering the surface charge and interfacial wettability of the particles, as evidenced by the zeta-potential. This phenomenon may enhance the repulsive forces between the droplets, resulting in the destructuion of any particle bridging [44].

3.8. Rheological properties

Most previous studies focused on the rheological properties of emulsions stabilized by small molecular emulsifiers or solid particles alone [37]. However, the influence of different NSMSs on the rheological properties of Pickering emulsions has been scarcely reported.

3.8.1. Apparent viscosity

As shown in Fig. 8A–C, the apparent viscosity (η) of all emulsions was gradually decreased with the increase in shear rate from 0.1 to 100 s^{-1}, indicating shear-thinning behaviour. The droplets tended to be distributed in a more orderly pattern along the flow field and offered less resistance to flow with lower viscosity when the shear rate was increased [32]. Due to the inappropriate wettability of the ZPCPs ($\theta o/w = 73.0 \pm 0.4°$), Z-P tended to form a more concentrated state, which was a type of particle-filled weak gel, and the network of aggregated droplets caused a higher viscosity [45]. In the presence of Rha, the apparent viscosity of the Pickering emulsions was decreased gradually and reached the minimum at Z-P/0.25rha (Fig. 8A). Considering the positive correlation between the viscosity of the emulsion and its physical stability, the addition of Rha at a low concentration had a detrimental effect on the stability of the Pickering emulsion. The competitive adsorption

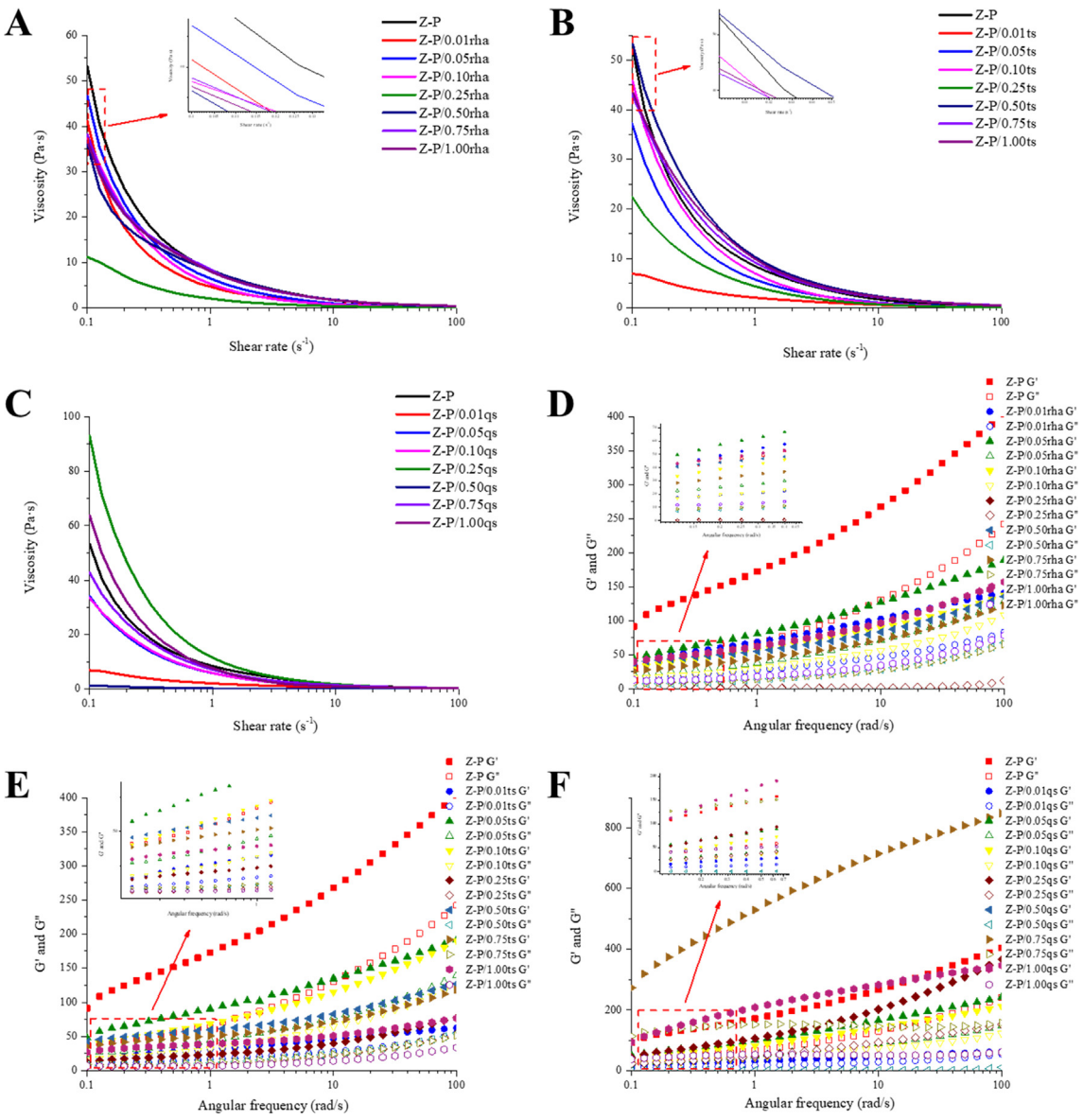

Fig. 8. Rheological properties of Pickering emulsions co-stabilized by ZPCPs and individual Rha (A, D), TS (B, E) or QS (C, F).

between Rha and ZPCPs weakened the interaction between the interfacial particles. Furthermore, the adsorption of Rha onto the surface of particles inhibited the bridging of particles between the droplets, thereby destroying the network formed by the particles at the interface. When the concentration of Rha was higher than 0.50% (w/v), the viscosity of the Pickering emulsion reversed to increase, indicating the formation of bridges by excessive Rha molecules adsorbed onto the surface of the droplets. The effect of different levels of TS on the viscosity of the Pickering emulsion was depicted in Fig. 8B. When TS was 0.01% (w/v), there was a huge declination in the viscosity of the Pickering emulsion, which demonstrated that TS exerted a greater interference on the interaction between the interfacial particles. As the concentration of TS was increased, the viscosity of the ZPCPs and TS co-stabilized Pickering emulsion was increased continuously, which was similar to Rha in forming the bridges among the droplets. The addition of QS had a more complex effect on the viscosity of the Pickering emulsion (Fig. 8C). Compared to Z-P, the addition of 0.01% (w/v) of QS reduced the viscosity of the Pickering emulsion, which was similar to the addition of TS. However, when the concentration of QS was increased from 0.05% to 0.25% (w/v), the viscosity of the ZPCPs and QS co-stabilized Pickering emulsion was markedly increased due to the bridging flocculation. At an intermediate concentration (0.50%, w/v), the viscosity of the Pickering emulsion suddenly reduced to the lowest point. The phenomenon was attributed to the fact that the adsorption of QS at the interface reduced the interfacial tension, which further lowered the viscosity of the Pickering emulsion. As the concentration of QS was further increased, the viscosity rose again, which was mainly attributable to the depletion effect caused by the excessive QS molecules between the droplets [12,42,43].

3.8.2. Viscoelastic properties

Dynamic frequency sweep tests were performed in the linear viscoelastic range to determine the frequency dependence of the storage modulus (G′) and loss modulus (G″). All of the emulsions showed that G′ was higher than G″ especially in Z-P, indicating that an elastic particulate gel-like structure was formed (Fig. 8D). The G′ was visibly decreased after the addition of Rha. The microstructure of the Pickering emulsion was formed by the bridging interaction between the particles adsorbed at the interface. The presence of Rha hindered the interaction between the particles and therefore

disrupted the elastic particulate solid-like structure. However, there was no noticeable difference in terms of the viscoelasticity of the Pickering emulsions at different concentrations of Rha. As the concentration of Rha increased, the G' of the Pickering emulsion decreased slightly.

A similar phenomenon was observed in the ZPCPs and TS co-stabilized Pickering emulsion. A marked reduction was observed in the relative values of G′ and G″ of the Pickering emulsion with the addition of TS. As the concentration of TS was increased, the G' of the Pickering emulsion decreased slightly and the gap between G' and G" was gradually reduced, which reflected a transition in the rheological properties of the Pickering emulsion from solid-like behaviour to liquid-like behaviour.

As shown in Fig. 8F, there was a gradual decrease in the G' of the ZPCPs and QS co-stabilized Pickering emulsion with the rise of QS level ranging from 0.05% to 0.50% (w/v). Nevertheless, the G' rose rapidly at a higher concentration of QS and reached a maximum at Z-P/0.75qs, which indicated the elastic-viscous-elastic transition in the rheological properties. This result revealed that a homogenous and stable Pickering emulsion could be generated at higher QS levels, potentially resulting from the excessive QS entanglement [39].

3.9. Environmental stability

3.9.1. pH

The pH stability of the Pickering emulsions was dependent on their interfacial compositions. Z-P/0.01rha was the most unstable among all the ZPCPs and Rha co-stabilized Pickering emulsions against pH fluctuation (Fig. 9A). When the concentration of Rha was greater than 0.25% (w/v), the droplet size of the Pickering emulsion was stable at different pH values. Besides, the droplet size of the Pickering emulsions decreased gradually with an increase in Rha levels. Although the negative charge of the emul-

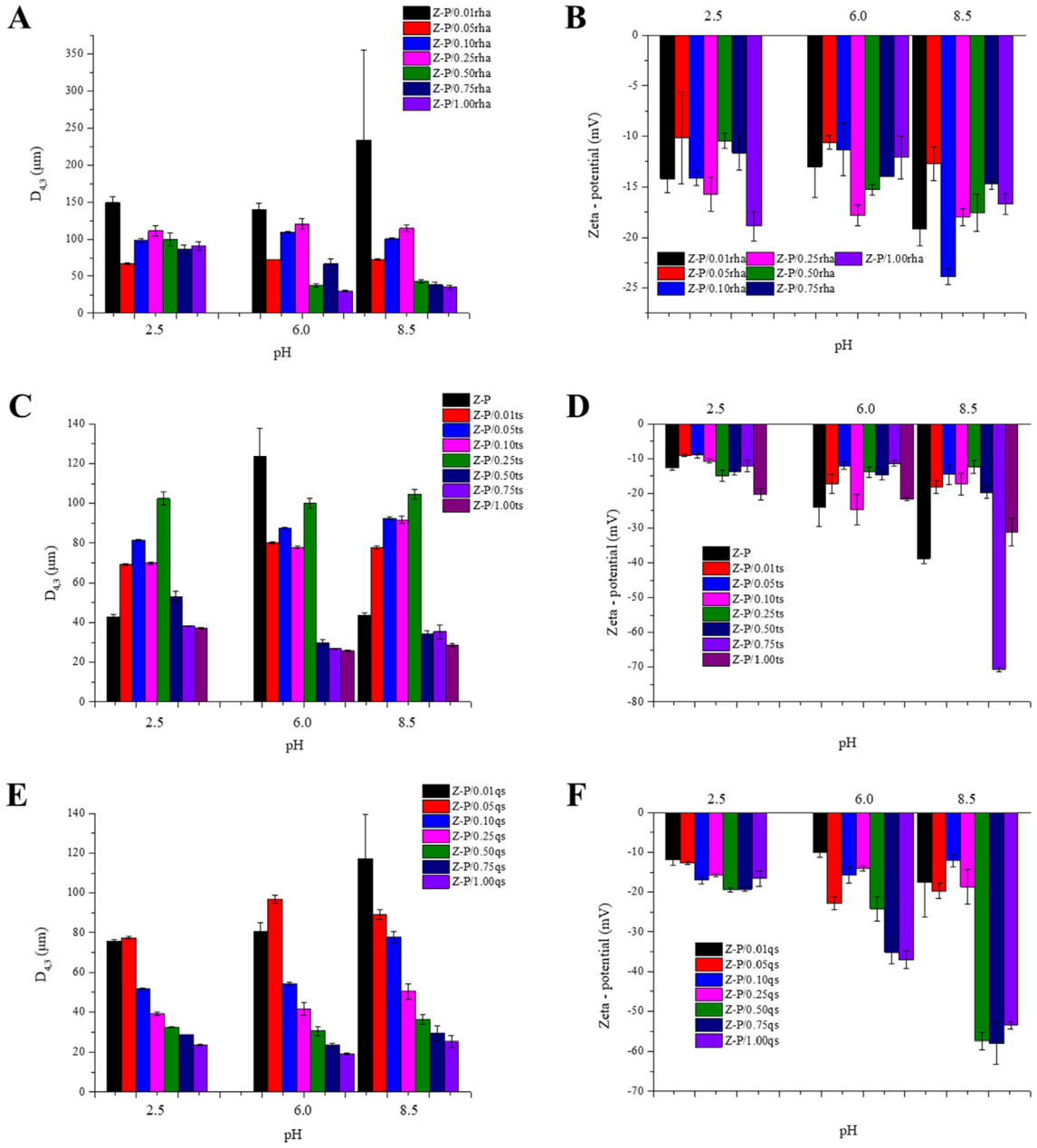

Fig. 9. Effect of pH on droplet size of Pickering emulsions co-stabilized by ZPCPs and Rha (A), TS (C) or QS (E), effect of pH on zeta-potential of Pickering emulsions co-stabilized by ZPCPs and individual Rha (B), TS (D) or QS (F).

sion under alkaline conditions was markedly more than that under neutral condition, the droplet size was not reduced in the presence of electrostatic repulsion (Fig. 9B). This result was consistent with that reported by previous studies [40].

Z-P was stable at pH 2.5 and 8.5, but unstable at pH 6.0, which was close to the pI value of zein (Fig. 9C) [24,25]. When TS was added at the intermediate concentration (0.50%, w/v), the ZPCPs and TS co-stabilized Pickering emulsion was more stable than Z-P in a neutral environment, but worsened under acidic and alkaline conditions. At pH 2.5, the zeta-potential of the ZPCPs and TS co-stabilized Pickering emulsion at lower concentrations of TS was lower than that of Z-P, which accounted for the coalescence of droplets (Fig. 9D). When TS was added at a higher concentration (>0.50%, w/v), the negative charge of the droplets was obviously increased due to carboxylic acid groups of TS [31,46,47]. Therefore, a sufficient electrostatic repulsion effectively improved the stability of the emulsion against pH fluctuation.

The ZPCPs and QS co-stabilized Pickering emulsion was unstable at different pH values at a low concentration of QS (Fig. 9E). As the concentration of QS was elevated continuously, the droplet size of the emulsion was decreased at different pHs. The increased amount of QS provided sufficient electrostatic repulsion between the droplets to reduce the droplet size (Fig. 9F). Nonetheless, the ZPCPs and QS co-stabilized Pickering emulsion exhibited the best stability under acidic conditions (pH 2.5) with the lowest negative charge compared to neutral and alkaline conditions, which was different from previous studies regarding the pH stability of the emulsions stabilized by QS alone [29,31]. Both ZPCPs and QS are negatively charged under acidic conditions, and therefore, the lowest electrostatic repulsion was observed between ZPCPs and QS at pH 2.5, due to the low negative charge. The reduction in repulsive force between the particles and surfactants either facilitated their co-adsorption onto the droplet surface to stabilize the emulsion or promoted the emulsifiers to be adsorbed onto the surface of particles to alter the wettability [42,44].

3.10. Ionic strength

Fig. 10A shows the effect of different levels of NaCl (0–100 mM) on the stability of the ZPCPs and Rha co-stabilized Pickering

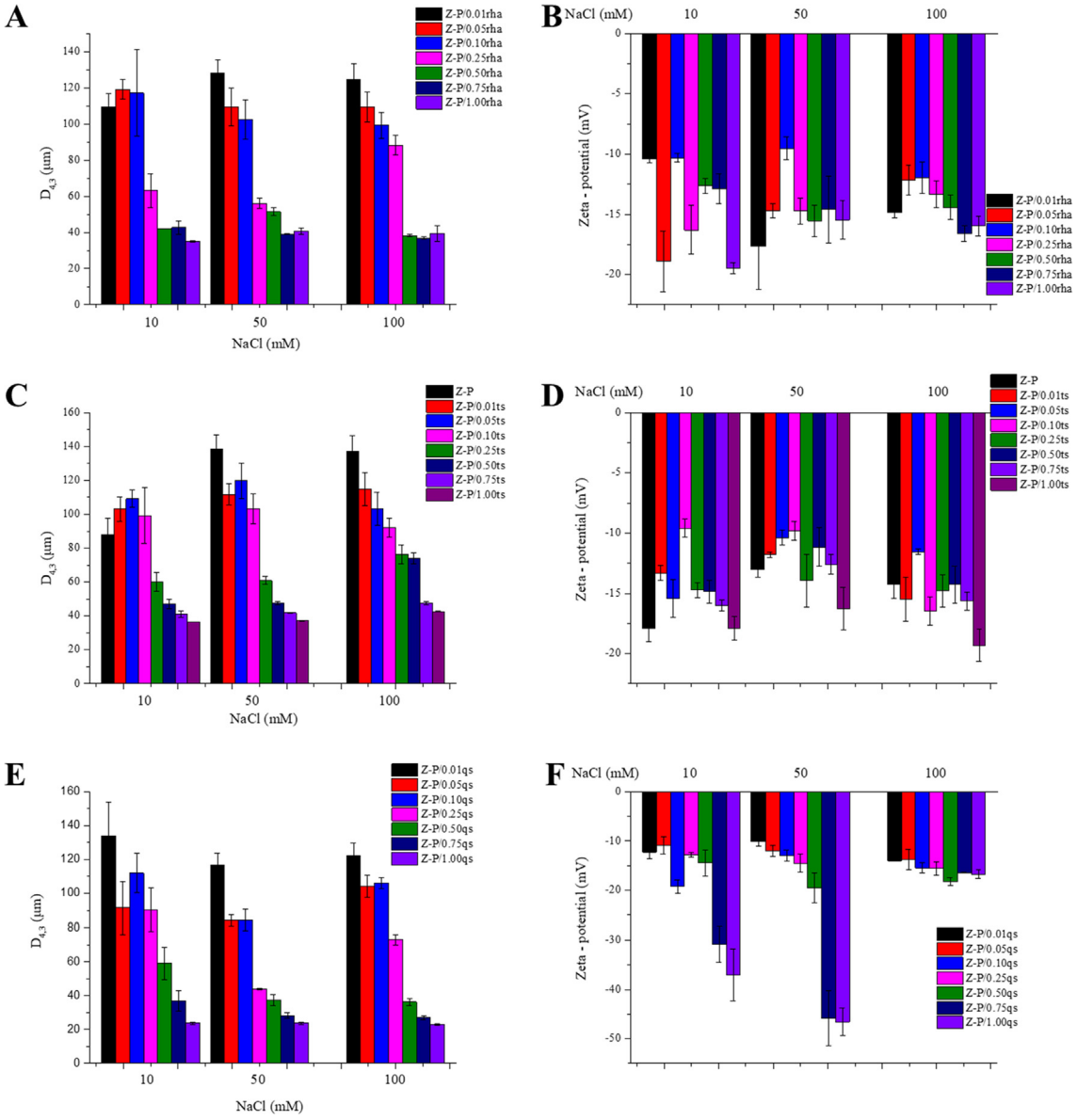

Fig. 10. Effect of ionic strength on droplet size of Pickering emulsions co-stabilized by ZPCPs and individual Rha (A), TS (C) or QS (E), effect of ionic strength on zeta-potential of Pickering emulsions co-stabilized by ZPCPs and individual Rha (B), TS (D) or QS (F).

emulsions. The droplet size was increased significantly ($p < 0.05$) in the presence of salt, especially at a low Rha concentration (<0.10%, w/v). When ionic strength was higher, the droplet size of the Pickering emulsion was stable. Although partial competitive displacement occurred at a higher Rha concentration, the remaining steric hindrance and electrostatic repulsion maintained the stability of the Pickering emulsion (Fig. 10B).

With the addition of TS, the Pickering emulsion was stable at a low level of salt (10 mM), but became unstable at an intermediate level of salt (50 mM) (Fig. 10C). This was attributed to the electrostatic screening with the rise of ionic strength, which accelerated the coalescence between the droplets (Fig. 10D). However, the droplet size remained constant when the level of NaCl was higher (100 mM), due to the steric hinderance provided by the interfacial layer.

There was an apparent increase in the droplet size of the ZPCPs and QS co-stabilized Pickering emulsion initially with an increased level of salt, followed by further small changes at higher salt levels (Fig. 10E). Particularly, the Pickering emulsion at a high concentration of QS (>0.50%, w/v) became very stable, although the negative charge of the droplets was significantly ($p < 0.05$) reduced at a high level of salt (100 mM) (Fig. 10F). These findings demonstrated that the instability of the Pickering emulsion co-stabilized by ZPCPs and QS at a higher level of salt was attributed to flocculation rather than coalescence, as a result of sufficient steric repulsion [12,39,42].

3.11. Thermal stability

The Pickering emulsions were heated at 85 °C for 60 min to evaluate their thermal stability. The Pickering emulsion stabilized by ZPCPs alone was found to be stable against heating (Fig. 11A). At a low concentration of Rha, the thermal stability of the Pickering emulsion was lower than that of Z-P. The droplet size of the ZPCPs and Rha co-stabilized Pickering emulsion was found to gradually increase with the rise of Rha concentration, indicating the coalescence of the oil droplets during thermal processing. However, when the Rha concentration was above 0.25% (w/v), the droplet size was found to continuously decrease with an increase in Rha levels. The emulsion was insensitive to heating when Rha was elevated, and thermal stability was enhanced. A similar phenomenon was observed in the ZPCPs and TS (Fig. 11B) or QS (Fig. 11C) co-stabilized Pickering emulsions. The thermal stability of the emulsion was effectively enhanced in the presence of surfactants at a high concentration. Among the three NSMSs, the Pickering emulsion with the addition of TS exhibited the best thermal stability. This result was mainly attributed to the fact that TS has a larger molecular weight, such that its adsorption onto the interface provided sufficient steric hindrance [41,42].

3.12. In vitro digestion fate of Pickering emulsions co-stabilized by particles and NSMSs

The digestion behaviour of novel Pickering emulsions in the simulated gastrointestinal tract was characterized by the droplet size and release of FFAs. A substantial increase in the droplet size of the Pickering emulsion stabilized by ZPCPs alone was observed after gastric digestion (Fig. 12A). The presence of pepsin may result in cross-linking between the adsorbed particles, followed by a severe aggregation of the droplets. Additionally, in a highly acidic environment, the negative charge of oil droplets was found to decrease sharply, and the electrostatic repulsion failed to prevent the aggregation of the droplets. After transferring to the intestinal phase, the droplet size was found to be markedly reduced due to the adsorption of bile salts, as well as an enhanced electrostatic repulsion. The presence of 0.10% (w/v) of Rha resulted in a more

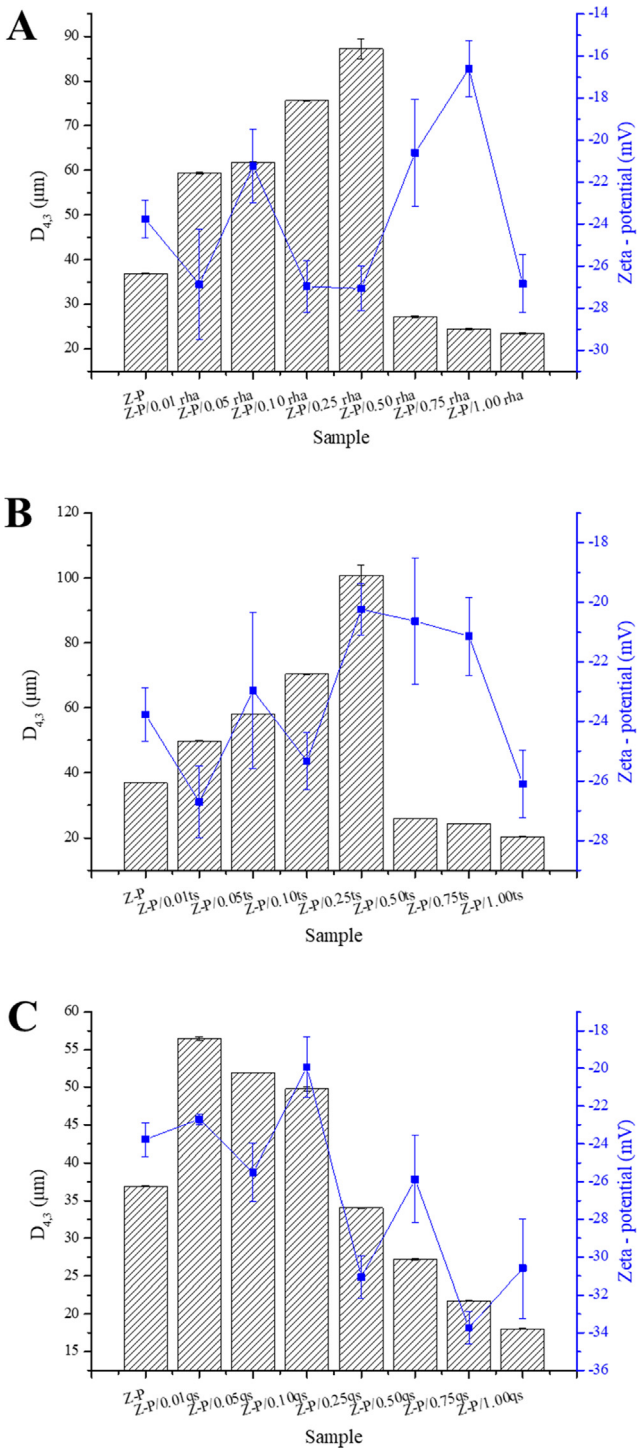

Fig. 11. Effect of thermal treatment on droplet size of Pickering emulsions co-stabilized by ZPCPs and individual Rha (A), TS (B) or QS (C).

serious flocculation of oil droplets in the gastric juice. However, the stability of the emulsion in the stomach was found to improve rapidly when the concentration of Rha was elevated. The presence of Rha effectively inhibited the aggregation of droplets in the gastric phase. A similar phenomenon was observed in the particles and TS or QS co-stabilized Pickering emulsions (Fig. 12 C and E). The Pickering emulsions with addition of NSMSs at a low concentration were very unstable in the gastric phase, with a droplet size that was increased appreciably. Conversely, the Pickering emulsions exhibited markedly better stability against coalescence at a

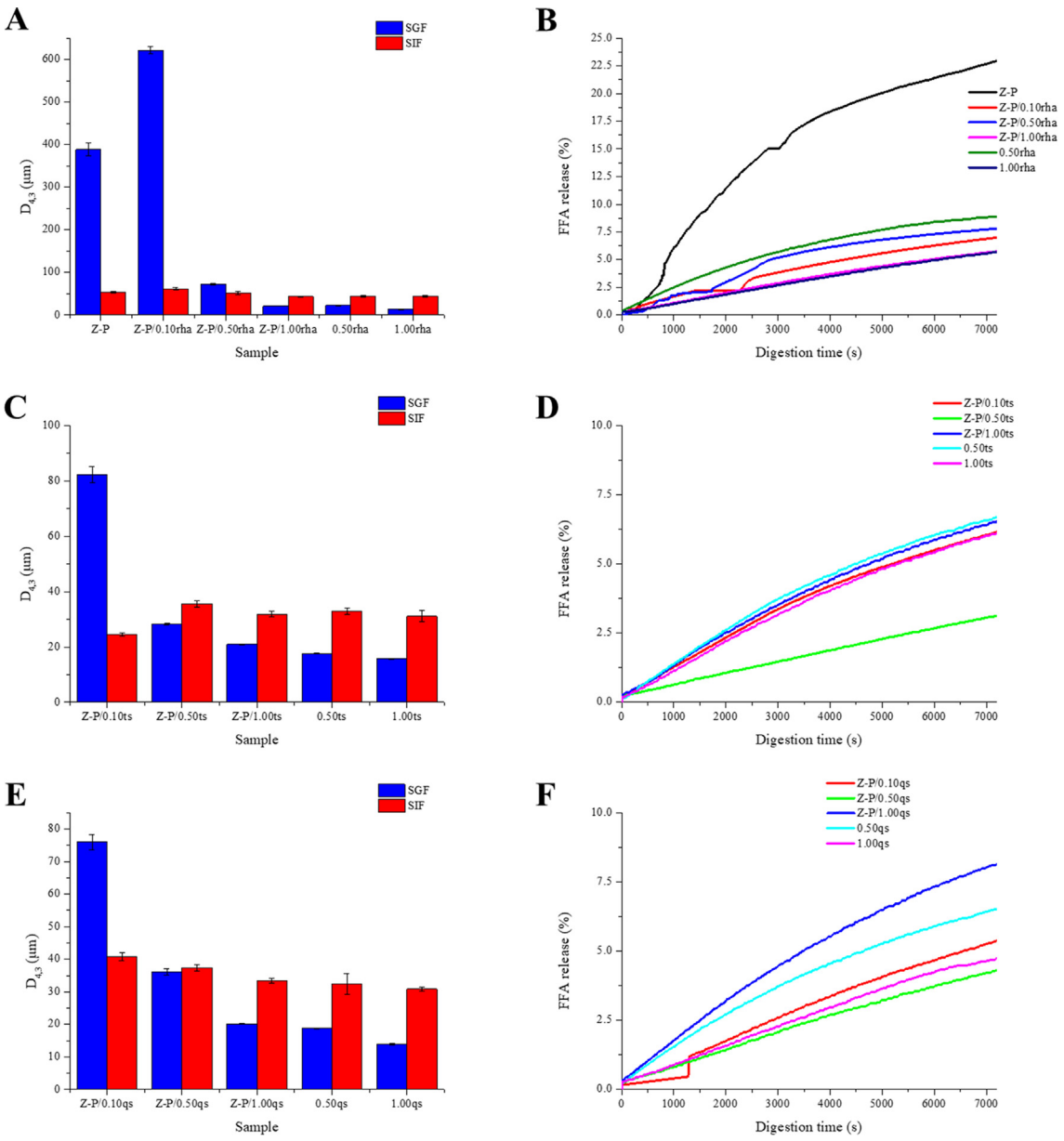

Fig. 12. Digestion time dependence of droplet size of the Pickering emulsions co-stabilized by ZPCPs and individual Rha (A), TS (C) or QS (E), digestion time dependence of FFA release (%) from Pickering emulsions co-stabilized by ZPCPs and individual Rha (B), TS (D) or QS (F).

higher concentration of NSMEs. After the emulsions were transferred into the small intestine from the stomach, the droplet size was found to increase. The stability of the Pickering emulsions during intestinal digestion was dependent on the digestive behaviour of the lipase [17,19]. The generation of surface-active free fatty acids (FFAs) and mono-acylglycerols (MAG) at the interface resulted in the coalescence of lipid droplets [21,39,48].

As the emulsion transcended from the stomach to intestine, the pH of the environment was adjusted from acidic to neutral.[49] The majority of the researchers in this field consider the key intestinal players to in the generation of FFAs from the hydrophobic lipid core with colipase to be bile salts and lipase [50,51]. As shown in Fig. 12B, Z-P exhibited the highest rate of FFA release (57.37%) after intestinal digestion for 2 h. Although the desorption energy of particles on the droplet surface was relatively large and difficult to be replaced by surfactants, the bile salts in the small intestine were still able to be adsorbed onto the interfacial gaps between the particles [14,18]. The successful adsorption of the bile salts at the interface facilitated the subsequent adsorption of lipase/colipase onto the surface of lipid droplets. However, the addition of Rha significantly ($p < 0.05$) reduced the FFA release rate of the Pickering emulsion. This was mainly attributed to the fact that Rha filled the remaining gaps between the particles, making it difficult for bile salts to be adsorbed onto the interface, which further inhibited lipid digestion. Fig. 12D showed the effect of TS concentration on the FFA release of the Pickering emulsion during intestinal digestion, whereby the addition of TS also inhibited the release of FFAs from the emulsion, similar to the addition of Rha. The main difference was that when Rha was added at an intermediate concentration (0.50%, w/v), the inhibition of lipolysis of the Pickering emulsion was stronger than that at a lower (0.10%, w/v) or higher (1.00%, w/v) concentration. However, the addition of TS at a low concentration resulted in it hardly being fully adsorbed by the gaps between ZPCPs, while the high concentration of TS may have resulted in the partial competitive displacement of particles, such that bile salts could be adsorbed onto the surface of lipid droplets. A similar phenomenon was observed in the ZPCPs and QS co-stabilized Pickering emulsion (Fig. 12F). Nevertheless,

the FFA release rate of Z-P/0.50qs (10.76%) was higher than that of Z-P/0.50ts (7.84%), indicating that the addition of TS at a level of 0.50% (w/v) into the Pickering emulsion had a better effect in delaying fat digestion. Our findings indicated that the design of O/W Pickering emulsions with a mixed particle/NSMS interface could effectively reduce the extent of lipid digestion in the small intestine, which could be applied in the development of novel fat substitutes for the enhancement of satiety, as well as for the delay of fat digestion.

4. Conclusion

In the present study, novel Pickering emulsions were fabricated using composite particles and different NSMSs (Rha, TS, and QS). The composite particles and NSMS were found to exhibit a synergetic behaviour in stabilizing the O/W emulsions. Among three types of NSMS, QS exhibited the best emulsifying capacity and reduced the interfacial tension more effectively than Rha and TS. CLSM was used to demonstrate that the morphology of the droplets changed from a spherical shape to a closely packed cell wall-like structure at extremely low levels of NSMS (0.01% and 0.05%, w/v). At higher levels of NSMS, the interfacial pores and inter-particle aggregation induced by competitive displacement were observed by cryo-SEM. Furthermore, the adsorption of NSMS onto the interface and the particle-NSMS interaction determined the rheological properties of the emulsions. In vitro digestion fate demonstrated that the particles and individual NSMSs at the intermediate concentration (0.50%, w/v) exerted a synergistic effect on inhibition of lipolysis during gastrointestinal digestion, highlighting its potential application in the development of novel fat replacers based on food colloids through interfacial design. Lastly, the novel Pickering emulsions could be utilized as a food delivery system to transport nutraceuticals and allow for their sustained release, improving their bioavailability *in vivo*.

Author contributions statement

Yang Wei: Conceptualization, Methodology, Software, Writing-Original draft preparation. **Zhen Tong:** Data curation. **Lei Dai:** Software. **Peihua Ma:** Investigation. **Mengfei Zhang:** Visualization. **Jinfang Liu:**Supervision. **Like Mao:** Software. **Fang Yuan:** Validation. **Yanxiang Gao:** Writing- Reviewing and Editing.

Declaration of Competing Interest

The authors declare that they have no known competing financial interests or personal relationships that could have appeared to influence the work reported in this paper.

Acknowledgement

The research was funded by the National Natural Science Foundation of China (No. 31871842). The authors are grateful to Tsinghua University Branch of China National Center Protein Sciences (Beijing, China) for providing the facility support of Cryo-SEM with the aid of Xiaomin Li.

Appendix A. Supplementary material

Supplementary data to this article can be found online at https://doi.org/10.1016/j.jcis.2019.12.085.

References

[1] D.E. Tambe, M.M. Sharma, The effect of colloidal particles on fluid-fluid interfacial properties and emulsion stability, Adv. Colloid Interface Sci. 52 (1994) 1–63, https://doi.org/10.1016/0001-8686(94)80039-1.
[2] B.P. Binks, S.O. Lumsdon, Influence of particle wettability on the type and stability of surfactant-free emulsions, Langmuir 16 (2000) 8622–8631, https://doi.org/10.1021/la000189s.
[3] J. Xiao, Y. Li, Q. Huang, Recent advances on food-grade particles stabilized Pickering emulsions: Fabrication, characterization and research trends, Trends Food Sci. Technol. 55 (2016) 48–60, https://doi.org/10.1016/J.TIFS.2016.05.010.
[4] E. Dickinson, Biopolymer-based particles as stabilizing agents for emulsions and foams, Food Hydrocoll. 68 (2017) 219–231, https://doi.org/10.1016/J.FOODHYD.2016.06.024.
[5] T. Review, Johnson Matthey Technol. Rev. (2015), https://doi.org/10.1016/0926-860X(93)85108-2.
[6] Y. Wei, C. Sun, L. Dai, L. Mao, F. Yuan, Y. Gao, Novel bilayer emulsions costabilized by zein colloidal particles and propylene glycol alginate, Part 1: Fabrication and characterization, J. Agric. Food Chem. 67 (2018) 1197–1208, https://doi.org/10.1021/acs.jafc.8b03240.
[7] B.P. Binks, Particles as surfactants—similarities and differences, Curr. Opin. Colloid Interface Sci. 7 (2002) 21–41, https://doi.org/10.1016/S1359-0294(02)00008-0.
[8] D. Eric, Colloidal Particles at Liquid Interfaces: Interfacial Particles in Food Emulsions and Foams, Cambridge University Press, Cambridge, 2006.
[9] Y. Wei, C. Sun, L. Dai, L. Mao, F. Yuan, Y. Gao, Novel bilayer emulsions costabilized by zein colloidal particles and propylene glycol alginate, Part 1: Fabrication and characterization, J. Agric. Food Chem. 67 (2019) 1197–1208, https://doi.org/10.1021/acs.jafc.8b03240.
[10] S. Zou, Y. Yang, H. Liu, C. Wang, Synergistic stabilization and tunable structures of Pickering high internal phase emulsions by nanoparticles and surfactants, Colloids Surfaces A Physicochem. Eng. Asp. 436 (2013) 1–9, https://doi.org/10.1016/J.COLSURFA.2013.06.013.
[11] J. Müller, K.N. Bauer, D. Prozeller, J. Simon, V. Mailänder, F.R. Wurm, S. Winzen, K. Landfester, Coating nanoparticles with tunable surfactants facilitates control over the protein corona, Biomaterials 115 (2017) 1–8, https://doi.org/10.1016/J.BIOMATERIALS.2016.11.015.
[12] M. Xu, J. Jiang, X. Pei, B. Song, Z. Cui, B.P. Binks, Novel oil-in-water emulsions stabilised by ionic surfactant and similarly charged nanoparticles at very low concentrations, Angew. Chemie - Int. Ed. 57 (2018) 7738–7742, https://doi.org/10.1002/anie.201802266.
[13] Z.-G. Cui, L.-L. Yang, Y.-Z. Cui, B.P. Binks, Effects of surfactant structure on the phase inversion of emulsions stabilized by mixtures of silica nanoparticles and cationic surfactant, Langmuir 26 (2009) 4717–4724, https://doi.org/10.1021/la903589e.
[14] B.P. Binks, J.A. Rodrigues, Double inversion of emulsions by using nanoparticles and a di-chain surfactant, Angew. Chemie - Int. Ed. 46 (2007) 5389–5392, https://doi.org/10.1002/anie.200700880.
[15] L. Wei, S. Yan, H. Wang, H. Yang, Fabrication of multi-compartmentalized mesoporous silica microspheres through a Pickering droplet strategy for enhanced CO2 capture and catalysis, NPG Asia Mater. 10 (2018) 899–911, https://doi.org/10.1038/s41427-018-0083-9.
[16] D. Liu, N. Xue, L. Wei, Y. Zhang, Z. Qin, X. Li, B.P. Binks, H. Yang, Surfactant assembly within pickering emulsion droplets for fabrication of interior-structured mesoporous carbon microspheres, Angew. Chemie - Int. Ed. 57 (2018) 10899–10904, https://doi.org/10.1002/anie.201805022.
[17] A. Sarkar, S. Zhang, M. Holmes, R. Ettelaie, Colloidal aspects of digestion of Pickering emulsions: experiments and theoretical models of lipid digestion kinetics, Adv. Colloid Interface Sci. 263 (2019) 195–211, https://doi.org/10.1016/j.cis.2018.10.002.
[18] S.R. Euston, W.G. Baird, L. Campbell, M. Kuhns, Competitive adsorption of dihydroxy and trihydroxy bile salts with whey protein and casein in oil-in-water emulsions, Biomacromolecules. 14 (2013) 1850–1858, https://doi.org/10.1021/bm4002443.
[19] A. Sarkar, B. Murray, M. Holmes, R. Ettelaie, A. Abdalla, X. Yang, In vitro digestion of Pickering emulsions stabilized by soft whey protein microgel particles: Influence of thermal treatment, Soft Matter. 12 (2016) 3558–3569, https://doi.org/10.1039/c5sm02998h.
[20] J. Maldonado-Valderrama, P. Wilde, A. Macierzanka, A. Mackie, The role of bile salts in digestion, Adv. Colloid Interface Sci. 165 (2011) 36–46, https://doi.org/10.1016/J.CIS.2010.12.002.
[21] Y. Xiao, C. Chen, B. Wang, Z. Mao, H. Xu, Y. Zhong, L. Zhang, X. Sui, S. Qu, In Vitro digestion of oil-in-water emulsions stabilized by regenerated chitin, J. Agric. Food Chem. 66 (2018) 12344–12352, https://doi.org/10.1021/acs.jafc.8b03873.
[22] R. Paliwal, S. Palakurthi, Zein in controlled drug delivery and tissue engineering, J. Control. Release 189 (2014) 108–122, https://doi.org/10.1016/J.JCONREL.2014.06.036.
[23] C. Sun, Y. Wei, R. Li, L. Dai, Y. Gao, Quercetagetin-loaded zein-propylene glycol alginate ternary composite particles induced by calcium ions: structure characterization and formation mechanism, J. Agric. Food Chem. 65 (2017) 3934–3945, https://doi.org/10.1021/acs.jafc.7b00921.
[24] Y. Wei, C. Sun, L. Dai, X. Zhan, Y. Gao, Structure, physicochemical stability and in vitro simulated gastrointestinal digestion properties of β-carotene loaded

zein-propylene glycol alginate composite nanoparticles fabricated by emulsification-evaporation method, Food Hydrocoll. 81 (2018) 149–158, https://doi.org/10.1016/j.foodhyd.2018.02.042.
[25] L. Dai, X. Zhan, Y. Wei, C. Sun, L. Mao, D.J. McClements, Y. Gao, Composite zein - propylene glycol alginate particles prepared using solvent evaporation: Characterization and application as Pickering emulsion stabilizers, Food Hydrocoll. 85 (2018) 281–290, https://doi.org/10.1016/J.FOODHYD.2018.07.013.
[26] L. Bai, D.J. McClements, Formation and stabilization of nanoemulsions using biosurfactants: rhamnolipids, J. Colloid Interface Sci. 479 (2016) 71–79, https://doi.org/10.1016/J.JCIS.2016.06.047.
[27] F. Müller, S. Hönzke, W.-O. Luthardt, E.L. Wong, M. Unbehauen, J. Bauer, R. Haag, S. Hedtrich, J. Rademann, Rhamnolipids form drug-loaded nanoparticles for dermal drug delivery, Eur. J. Pharm. Biopharm. 116 (2017) 31–37, https://doi.org/10.1016/J.EJPB.2016.12.013.
[28] C.L. Reichert, H. Salminen, J. Weiss, Quillaja saponin characteristics and functional properties, Annu. Rev. Food Sci. Technol. 10 (2019) 43–73, https://doi.org/10.1146/annurev-food-032818-122010.
[29] Y. Yang, M.E. Leser, A.A. Sher, D.J. McClements, Formation and stability of emulsions using a natural small molecule surfactant: Quillaja saponin (Q-Naturale®), Food Hydrocoll. 30 (2013) 589–596, https://doi.org/10.1016/J.FOODHYD.2012.08.008.
[30] Z. Li, L. Dai, D. Wang, L. Mao, Y. Gao, Stabilization and rheology of concentrated emulsions using the natural emulsifiers quillaja saponins and rhamnolipids, J. Agric. Food Chem. 66 (2018) 3922–3929, https://doi.org/10.1021/acs.jafc.7b05291.
[31] Z. Zhu, Y. Wen, J. Yi, Y. Cao, F. Liu, D.J. McClements, Comparison of natural and synthetic surfactants at forming and stabilizing nanoemulsions: Tea saponin, Quillaja saponin, and Tween 80, J. Colloid Interface Sci. 536 (2019) 80–87, https://doi.org/10.1016/j.jcis.2018.10.024.
[32] C. Sun, S. Gunasekaran, M.P. Richards, Effect of xanthan gum on physicochemical properties of whey protein isolate stabilized oil-in-water emulsions, Food Hydrocoll. 21 (2007) 555–564, https://doi.org/10.1016/J.FOODHYD.2006.06.003.
[33] Y. Wei, L. Zhang, Z. Yu, K. Lin, S. Yang, L. Dai, J. Liu, L. Mao, F. Yuan, Y. Gao, Enhanced stability, structural characterization and simulated gastrointestinal digestion of coenzyme Q10 loaded ternary nanoparticles, Food Hydrocoll. 94 (2019) 333–344, https://doi.org/10.1016/j.foodhyd.2019.03.024.
[34] J. O'Sullivan, M. Arellano, R. Pichot, I. Norton, The effect of ultrasound treatment on the structural, physical and emulsifying properties of dairy proteins, Food Hydrocoll. 42 (2014) 386–396, https://doi.org/10.1016/J.FOODHYD.2014.05.011.
[35] L. Dai, C. Sun, Y. Wei, L. Mao, Y. Gao, Characterization of Pickering emulsion gels stabilized by zein/gum arabic complex colloidal nanoparticles, Food Hydrocoll. 74 (2018) 239–248, https://doi.org/10.1016/J.FOODHYD.2017.07.040.
[36] P. Sriamornsak, N. Thirawong, K. Cheewatanakornkool, K. Burapapadh, W. Sae-Ngow, Cryo-scanning electron microscopy (cryo-SEM) as a tool for studying the ultrastructure during bead formation by ionotropic gelation of calcium pectinate, Int. J. Pharm. 352 (2008) 115–122, https://doi.org/10.1016/J.IJPHARM.2007.10.038.
[37] Y. Wei, C. Sun, L. Dai, L. Mao, F. Yuan, Y. Gao, Novel bilayer emulsions costabilized by zein colloidal particles and propylene glycol alginate. 2. Influence of environmental stresses on stability and rheological properties, J. Agric. Food Chem. 67 (2019) 1209–1221, https://doi.org/10.1021/acs.jafc.8b04994.
[38] Y. Li, D. Julian McClements, New mathematical model for interpreting pH-stat digestion profiles: impact of lipid droplet characteristics on in vitro digestibility, J. Agric. Food Chem. 58 (2010) 8085–8092, https://doi.org/10.1021/jf101325m.
[39] B.P. Binks, A. Desforges, D.G. Duff, Synergistic stabilization of emulsions by a mixture of surface-active nanoparticles and surfactant, Langmuir 23 (2007) 1098–1106, https://doi.org/10.1021/la062510y.
[40] R.B. Lovaglio, F.J. dos Santos, M. Jafelicci, J. Contiero, Rhamnolipid emulsifying activity and emulsion stability: pH rules, Colloids Surfaces B Biointerfaces. 85 (2011) 301–305, https://doi.org/10.1016/J.COLSURFB.2011.03.001.
[41] P. Wilde, A. Mackie, F. Husband, P. Gunning, V. Morris, Proteins and emulsifiers at liquid interfaces, Adv. Colloid Interface Sci. 108–109 (2004) 63–71, https://doi.org/10.1016/J.CIS.2003.10.011.
[42] A. Mackie, P. Wilde, The role of interactions in defining the structure of mixed protein–surfactant interfaces, Adv. Colloid Interface Sci. 117 (2005) 3–13, https://doi.org/10.1016/J.CIS.2005.04.002.
[43] L.A. Pugnaloni, E. Dickinson, R. Ettelaie, A.R. Mackie, P.J. Wilde, Competitive adsorption of proteins and low-molecular-weight surfactants: computer simulation and microscopic imaging, Adv. Colloid Interface Sci. 107 (2004) 27–49, https://doi.org/10.1016/J.CIS.2003.08.003.
[44] D.J. French, P. Taylor, J. Fowler, P.S. Clegg, Making and breaking bridges in a Pickering emulsion, J. Colloid Interface Sci. 441 (2015) 30–38, https://doi.org/10.1016/J.JCIS.2014.11.032.
[45] E. Dickinson, Emulsion gels: the structuring of soft solids with protein-stabilized oil droplets, Food Hydrocoll. 28 (2012) 224–241, https://doi.org/10.1016/J.FOODHYD.2011.12.017.
[46] S. Böttcher, S. Drusch, Saponins – self-assembly and behavior at aqueous interfaces, Adv. Colloid Interface Sci. 243 (2017) 105–113, https://doi.org/10.1016/J.CIS.2017.02.008.
[47] S. Uluata, D. Julian McClements, E.A. Decker, Physical stability, autoxidation, and photosensitized oxidation of ω-3 oils in nanoemulsions prepared with natural and synthetic surfactants, J. Agric. Food Chem. 63 (2015) 9333–9340, https://doi.org/10.1021/acs.jafc.5b03572.
[48] A. Sarkar, A. Ye, H. Singh, On the role of bile salts in the digestion of emulsified lipids, Food Hydrocoll. 60 (2016) 77–84, https://doi.org/10.1016/J.FOODHYD.2016.03.018.
[49] H. Singh, A. Ye, Structural and biochemical factors affecting the digestion of protein-stabilized emulsions, Curr. Opin. Colloid Interface Sci. 18 (2013) 360–370, https://doi.org/10.1016/J.COCIS.2013.04.006.
[50] H. Brockman, Colipase-induced reorganization of interfaces as a regulator of lipolysis, Colloids Surfaces B Biointerfaces 26 (2002) 102–111, https://doi.org/10.1016/S0927-7765(02)00031-0.
[51] H. van Tilbeurgh, S. Bezzine, C. Cambillau, R. Verger, F. Carrière, Colipase: structure and interaction with pancreatic lipase, Biochim. Biophys. Acta - Mol. Cell Biol. Lipids. 1441 (1999) 173–184, https://doi.org/10.1016/S1388-1981(99)00149-3.